

Decoupling of large-scale, adiabatic inflationary perturbations from enhanced small-scale modes at one-loop

Laura Iacconi  ^{1,2} **David Mulryne**,¹ **David Seery**  ³

¹Astronomy Unit, Queen Mary University of London,
Mile End Road, London, E1 4NS, UK

²Institute of Cosmology and Gravitation, University of Portsmouth,
Burnaby Road, Portsmouth, PO1 3FX, UK

³Astronomy Centre, University of Sussex,
Falmer, Brighton, BN1 9QH, UK

E-mail: l.iacconi@qmul.ac.uk, d.mulryne@qmul.ac.uk, D.Seery@sussex.ac.uk

Abstract. We reconsider back-reaction from large amplitude, short-scale perturbations onto a long wavelength adiabatic mode. In a loop expansion of the long-mode power spectrum, this back-reaction appears first at 1-loop. Due to the separation between the long and short scales, the separate universe method provides a simple and efficient framework for this computation. In this paper, building on our earlier work, we employ a δN formula for the long mode, which captures the effect of short scales. We show that back-reaction at 1-loop is due to either (i) non-linearity of the δN formula, or (ii) 1-loop corrections to the initial conditions. We argue that contributions of type (ii) cannot themselves be described within the separate universe framework, but their properties can be constrained using soft theorems and a “multi-point propagator” expansion. When applied to a band of enhanced short-scale perturbations that crossed the horizon during inflation, our result shows that the loop correction decouples from their detailed properties. Furthermore, the back-reaction we obtain is scale-invariant. Its magnitude is model-dependent, but is degenerate with effects from modes that were still sub-horizon at the end of inflation. In this scenario (but not necessarily in all scenarios), we conclude that the effect is not observable.

Contents

1	Introduction	2
1.1	Roadmap	3
1.2	Conventions and definitions	3
2	Properties of long and short modes	5
3	Loops in the separate universe framework	7
3.1	The separate universe framework	7
3.2	The separate universe framework for models with a non-attractor phase	9
3.3	Correlation functions	12
3.4	Does the separate universe framework capture “in–in” loop effects?	14
3.5	The 1-loop contributions	17
4	1-loop from non-linear superhorizon evolution is a boundary term	19
4.1	Combining the (12)- and (13)-type loops	19
4.2	Interpretation and discussion	22
5	The (11)-type loop is a boundary term	27
5.1	The (11)-type loop	28
5.2	Lessons from the loop computation	32
5.3	Renormalized δN coefficients	33
6	Discussion	35
A	Tree-level application of separate universe to a ultra-slow-roll model	38
B	Squeezed phase-space bispectrum some e-folds after horizon crossing	40

1 Introduction

Recently there has been much interest in evaluation of loop corrections to the correlation functions of the inflationary curvature perturbation ζ . These corrections are interesting because (among other effects), at each scale, they measure back-reaction due to structure on much shorter scales [1, 2]. At small wavenumbers, the statistics of the curvature perturbation are tightly constrained by CMB and galaxy-clustering observations, and are consistent with tree-level predictions from single-field, slow-roll inflation. To maintain this success, the backreaction onto these wavenumbers should not disrupt their statistical properties. This may be a nontrivial constraint. In scenarios where the amplitude of short-scale fluctuations is enhanced (for example, to produce a population of early compact objects such as primordial black holes), there is a reasonable concern that significant back-reaction may occur.

Estimates of the back-reaction effect have been obtained at 1-loop level. However, its amplitude continues to be debated in the literature [1–33]. Kristiano & Yokoyama [5] studied the case of a transient ultra-slow-roll (USR) phase [34–36] in a single-field model. This is sometimes regarded as a possible scenario leading to primordial black hole (PBH) production. They estimated that an enhancement of small-scale power sufficient to produce interesting abundances of PBHs could induce a 1-loop power spectrum comparable to the tree-level one, which we would usually interpret to mean that backreaction effects were not under adequate control. The amplitude of their effect was proportional to the peak amplitude of the short-scale power spectrum.

Kristiano & Yokoyama worked in a simplified model designed for analytic treatment. Their work was followed by many authors, who attempted to obtain refined estimates by relaxing assumptions made in Ref. [5], or by accounting for extra physical effects. Like many subsequent authors, they made use of the “in–in” formalism of nonequilibrium quantum field theory, and in particular its diagrammatic expansion into Green’s functions. This is powerful, but complicated. Some—but, as we shall see, usually not all—of the back-reaction we wish to capture takes place when quantum effects are not significant. This suggests that it may be possible to simplify the calculation by replacing the Green’s function approach with a classical procedure.

In an earlier paper, Ref. [2], we suggested that it should be possible to use the separate universe framework to build a classical back-reaction model.¹ In particular, we studied the back-reaction onto long-wavelength modes with wavenumber p from ultra-slow-roll scales, near wavenumber q . In common with many similar processes characterized by decoupling and separation of scales, there is an EFT-like description expressed in terms of effects entering at different powers of p/q . In Ref. [2] we evaluated the different 1-loop contributions due to non-linear super-horizon evolution, finding one which was volume-suppressed (i.e., scaling as $(p/q)^3$), and two which were unsuppressed. The unsuppressed effects are supported by long–short mode couplings [2].

In this paper we return to the topic of back-reaction, building on the results of Ref. [2]. Our aim is now to include effects from a broad band of enhanced fluctuations. For realistic

¹See also Ref. [10] for an earlier application of the δN framework, although the details differ from those of Ref. [2].

models this is usually represented by a localized peak in $\mathcal{P}_{\zeta, \text{tree}}$, including modes rising to and falling away from the main peak. Further, we account for 1-loop contributions in the initial conditions of the separate universe computation, which were not included in Ref. [2]. After dropping volume-suppressed contributions at 1-loop, we investigate the mathematical structure of the remaining effects. The result yields a compact and illuminating final expression. We use this to assess under what conditions a broad peak can lead to observable effects on larger scales, and whether the importance of these effects depends on the peak amplitude, as concluded in Ref. [5].

Our analysis depends on two fundamental assumptions. These are that: (i) the field configuration described by the long mode is adiabatic, and (ii) there is sufficient separation of scales between the long mode and the short scales whose effect we want to capture. Assumption (ii) is needed to allow the application of soft theorems to determine the response of short-scale correlation functions to the long-wavelength mode. Apart from the assumption that these soft theorems are themselves valid, no further assumptions are made, e.g. regarding the nature of the transient non-attractor phase, or the type and duration of the transitions into and out of this phase. To make contact with the literature, we sometimes give explicit expressions for the case of a transient USR era. However, our discussion is not limited to this scenario. Our analysis is applicable to any single-field model which realizes assumptions (i) and (ii). Finally, although we focus on the case of single-field inflation, we briefly discuss the applicability of our results to more general scenarios in §6.

1.1 Roadmap

In §2 we briefly summarize the properties of the long mode for which we wish to estimate the change due to back-reaction, and of the short-scale modes that induce the effect. We spell out the two fundamental assumptions of adiabaticity of the long mode, and separation of scales. These provide the foundation for the remainder of our analysis.

In §3.1 we review the separate universe framework. We comment on its application to models containing a sudden deviation from slow-roll dynamics in §3.2. In §3.3 we review the δN formula including back-reaction, and explain how it can be used to compute the long-mode power spectrum at 1-loop [2]. In §3.4 we argue that the loops computed by applying separate universe capture the same effects as “in–in” loop integrals (at least for the specific computation of interest here), and discuss the correct choice of the δN initialization time. In §3.5 we collect all 1-loop contributions, and distinguish between those where the loop is due to (i) non-linearity of the δN formula, or (ii) initial conditions at 1-loop.

We present our main computations in §4 and §5. For both cases (i) (in §4) and (ii) (in §5) we show that the non-volume-suppressed contributions can be written in a compact form, where the integrand is the total derivative of a function whose explicit form we provide. We conclude in §6 by discussing the implications of our results. In Appendix A and B we provide additional materials.

1.2 Conventions and definitions

We work in natural units where $c = \hbar = 1$. The reduced Planck mass is defined by $M_P = (8\pi G)^{-1/2}$, where G is Newton’s gravitational constant.

Phase space.—For a generic inflation model with M fields, we collect the fields and their momenta into a $2M$ -dimensional phase-space vector

$$X^I(\mathbf{x}, t) \equiv (\phi^1(\mathbf{x}, t), \dots, \phi^M(\mathbf{x}, t), \pi^1(\mathbf{x}, t), \dots, \pi^M(\mathbf{x}, t)), \quad (1.1)$$

where $\pi \equiv \phi'$, and a prime ' indicates a derivative with respect to the e-fold number N , defined by $dN \equiv Hdt$. Latin indices I, J, \dots run over $1, \dots, 2M$ and label phase-space coordinates. Each phase-space coordinate can be decomposed into a background component and a linear perturbation, viz., $X^I(\mathbf{x}, t) = \bar{X}^I(t) + \delta X^I(\mathbf{x}, t)$.

Fourier transforms.—Our Fourier transform convention is

$$f(\mathbf{k}) = \int d^3x f(\mathbf{x}) e^{-i\mathbf{k}\cdot\mathbf{x}} \quad \text{and} \quad f(\mathbf{x}) = \int \frac{d^3k}{(2\pi)^3} f(\mathbf{k}) e^{i\mathbf{k}\cdot\mathbf{x}},$$

where $f(\mathbf{x})$ and $f(\mathbf{k})$ represent an arbitrary function and its Fourier transform, respectively. We sometimes use the shorter notation $f_{\mathbf{k}} = f(\mathbf{k})$, or $[\mathcal{O}]_{\mathbf{k}}$ for the Fourier mode of a composite quantity \mathcal{O} .

Wavevectors.—We use \mathbf{p} to label the comoving wavevector of a long mode, and \mathbf{q} to label the wavevectors of enhanced short modes. The back-reaction effect we aim to compute is a measure of the aggregate effect \mathbf{q} -modes have on the longer \mathbf{p} -mode. If there is a band of enhanced short-scale modes, rather than a single well-defined mode, we use k_{peak} to label the most strongly enhanced mode.

In single field models with a non-attractor phase, we use t_s and t_e to label the start and end times of the non-attractor behaviour. The corresponding scales crossing the horizon at these times are k_s and k_e , where (as usual) the horizon-crossing time t_k for a scale k is defined by the condition $k = (aH)_{t=t_k}$.

Correlation functions.—We define the spectrum P_{ζ} and bispectrum B_{ζ} for the curvature perturbation ζ in terms of the equal-time 2- and 3-point correlation functions,

$$\langle \zeta_{\mathbf{k}_1}(t) \zeta_{\mathbf{k}_2}(t) \rangle \equiv (2\pi)^3 \delta(\mathbf{k}_1 + \mathbf{k}_2) P_{\zeta}(k_1; t), \quad (1.2a)$$

$$\langle \zeta_{\mathbf{k}_1}(t) \zeta_{\mathbf{k}_2}(t) \zeta_{\mathbf{k}_3}(t) \rangle \equiv (2\pi)^3 \delta(\mathbf{k}_1 + \mathbf{k}_2 + \mathbf{k}_3) B_{\zeta}(k_1, k_2, k_3; t). \quad (1.2b)$$

The spectrum and bispectrum depend only on the magnitudes of their wavevector arguments, and not their orientation, as a consequence of statistical translation invariance and isotropy.

We also define a dimensionless power spectrum and a reduced (dimensionless) bispectrum,

$$\mathcal{P}_{\zeta}(k; t) \equiv \frac{k^3}{2\pi^2} P_{\zeta}(k; t), \quad (1.3a)$$

$$f_{\text{NL}}(k_1, k_2, k_3; t) \equiv \frac{5}{6} \frac{B_{\zeta}(k_1, k_2, k_3; t)}{P_{\zeta}(k_1; t) P_{\zeta}(k_2; t) + P_{\zeta}(k_1; t) P_{\zeta}(k_3; t) + P_{\zeta}(k_2; t) P_{\zeta}(k_3; t)}. \quad (1.3b)$$

Finally, we introduce equal-time 2- and 3-point correlation functions in phase space

$$\langle \delta X_{\mathbf{k}_1}^I(t) \delta X_{\mathbf{k}_2}^J(t) \rangle \equiv (2\pi)^3 \delta(\mathbf{k}_1 + \mathbf{k}_2) P^{IJ}(k_1; t), \quad (1.4a)$$

$$\langle \delta X_{\mathbf{k}_1}^I(t) \delta X_{\mathbf{k}_2}^J(t) \delta X_{\mathbf{k}_3}^K(t) \rangle \equiv (2\pi)^3 \delta(\mathbf{k}_1 + \mathbf{k}_2 + \mathbf{k}_3) \alpha^{IJK}(k_1, k_2, k_3; t). \quad (1.4b)$$

2 Properties of long and short modes

Our objective is to investigate back-reaction onto a large-scale mode \mathbf{p} , due to small-scale modes with enhanced amplitude and typical wavenumbers of order q . We usually have in mind a scenario where \mathbf{p} contributes to the CMB anisotropy or the statistics of galaxy clustering, and therefore is constrained by observation. However, our results are more general and require only a separation of scales, so that $p \ll q$. We write the horizon exit time for \mathbf{p} as t_p , and the horizon exit time for a typical enhanced mode as t_q . Eventually we are interested in the scenario where a broad band of modes near q are enhanced, in which case t_q may not be well defined. However, here and below, we use this notation where it simplifies the presentation, but our analysis does not depend on it.

We focus on single-field models. In such scenarios, enhanced small-scale fluctuations can be produced when slow-roll evolution is temporarily interrupted by an ultra-slow-roll phase² (where $\epsilon_1 \ll 1$ and $\epsilon_2 \sim -6$), or by other non-attractor dynamics. Here, $\epsilon_1 \equiv -H'/H$, $\epsilon_2 \equiv \epsilon'_1/\epsilon_1$, and a prime $'$ denotes a derivative with respect to $dN = H dt$. The non-attractor phase is itself assumed to be followed by another era, which may be a second slow-roll period or something else. The mode \mathbf{p} crosses the horizon during the first slow-roll period. In §6 we comment briefly on the applicability of our results to more general scenarios, including multiple-field models.

In this section we review the physical properties of the small- and large-scale modes. We assume these are coupled by long–short correlations that control how small scales respond to changes in the long-wavelength fields. As explained in §1, we have two main requirements: (i) the long-wavelength configuration is *adiabatic*; and (ii) there is an appreciable separation of scales, so that the short-scale fields experience the long-wavelength disturbance as a nearly-constant shift. We now consider each of these conditions in more detail.

Long-wavelength disturbance is adiabatic.—The long-wavelength mode \mathbf{p} will typically pass outside the horizon some time before any enhanced short-scale perturbations. In certain models the corresponding field configuration may be adiabatic, in the sense that the perturbation in each relevant field (or their momenta) at wavenumber \mathbf{p} is derived from a shift along the background trajectory. Here, “relevant” means that the field carries a non-negligible fraction of the cosmological energy budget.

In a single-field (or effectively single-field) model the condition of adiabaticity entails further simplifications. The relevant phase space (1.1) will be spanned by some field-space direction ϕ and its momentum π . For the models we will consider, the adiabatic condition relates $\delta\pi$ to $\delta\phi$ via

$$\delta\pi_{\mathbf{p}}(t) = \frac{\epsilon_2}{2} \delta\phi_{\mathbf{p}}(t) + \text{decaying}, \quad (t > t_p) \quad (2.1)$$

where the perturbations $\delta\phi$, $\delta\pi$ are defined on spatially flat hypersurfaces. Eq. (2.1) is valid after horizon crossing, once decaying contributions can be neglected. Note that this includes smooth transitions between the different dynamical phases.

The condition (2.1) guarantees that $\delta\phi$ and $\delta\pi$ combine to displace the field configuration along the *original* phase space trajectory. In any region where the evolution of the field value

²Notice that, despite the name, ultra-slow-roll is *not* a sub-case of slow-roll.

ϕ is monotonic, we can choose to measure position along this trajectory using ϕ . The rate of change of any phase-space function $F(\phi, \pi)$ on the trajectory can then be obtained using the usual advective derivative,

$$\frac{d}{d\phi} \equiv \frac{\partial}{\partial\phi} + \frac{\epsilon_2}{2} \frac{\partial}{\partial\pi} . \quad (2.2)$$

Eq. (2.2) will play an important role in the emergence of a total derivative in the 1-loop computation. (See §4.1.)

Reaction of short-scale perturbations.—Some time after horizon exit of \mathbf{p} (perhaps a very long time afterwards), the enhanced short-scale perturbations exit the horizon. We take this to happen at time $t \sim t_q$. The short modes exit into a background that is locally disturbed by the long-wavelength \mathbf{p} -mode. Because of the hierarchy of scales, modes with wavenumbers in the vicinity of q experience this disturbance as a nearly-constant shift in the background fields and their momenta.

We now collect ϕ and π into a single vector X^L . For a pure shift δX^L in the background fields we could evaluate the response of the 2-point function via a Taylor expansion [37–39]

$$\langle \delta X_{\mathbf{q}}^I \delta X_{-\mathbf{q}}^J \rangle'_t = \langle \delta X_{\mathbf{q}}^I \delta X_{-\mathbf{q}}^J \rangle'_t \Big|_0 + \frac{\partial \langle \delta X_{\mathbf{q}}^I \delta X_{-\mathbf{q}}^J \rangle'_t}{\partial X^L(t)} \Big|_0 \delta X^L(t) + \dots , \quad (2.3)$$

where “ \dots ” denotes corrections of higher orders in δX^L . The notation $|_0$ indicates that the attached quantity is to be evaluated in the absence of the background disturbance, and $\langle \dots \rangle_t$ denotes an equal-time correlation function evaluated at time t . Finally, a prime ‘ attached to a correlation function indicates that factors of $(2\pi)^3$ and the momentum conservation δ -function should be removed. Similar expressions can be written for each higher correlation function.

Long-short mode coupling.—We can regard Eq. (2.3) as a simple example of an operator product expansion. This determines the behaviour of the composite operator $\delta X^I \delta X^J$ when correlated with perturbations at wavenumbers much smaller than q . Promoting (2.3) in this way, we obtain the operator relation [38–40]

$$\delta X_{\mathbf{q}}^I \delta X_{\mathbf{p}-\mathbf{q}}^J \Big|_t \approx (2\pi)^3 \delta(\mathbf{p}) \langle \delta X_{\mathbf{q}}^I \delta X_{-\mathbf{q}}^J \rangle'_t \Big|_0 + \frac{\partial \langle \delta X_{\mathbf{q}}^I \delta X_{-\mathbf{q}}^J \rangle'_t}{\partial X^L(t)} \Big|_0 \delta X_{\mathbf{p}}^L(t) + \dots . \quad (2.4)$$

Here, “ \dots ” takes the place of the higher-order corrections in (2.3), and now indicates all omitted higher-dimensional operators. We assume these to be defined so that they have zero expectation value. In addition to higher powers of the perturbations δX^L , which would already appear in the Taylor expansion (2.3), the omitted operators will include gradients such as $\partial^2 \delta X_{\mathbf{p}}^L$ that introduce corrections of order p^2 . We will shortly consider the significance of these. The symbol \approx denotes a weak equality, in the sense that Eq. (2.4) should be regarded as valid when used inside a correlation function. However, Eq. (2.4) is expected to hold as an *operator* statement. Therefore, the same expansion can be used in any correlation function.

The operator product expansion controls all long–short correlations [41, 42]. One important and familiar example controls the “squeezed” limit of the three-point function

$\langle \delta X_{\mathbf{p}} \delta X_{\mathbf{q}} \delta X_{-\mathbf{p}-\mathbf{q}} \rangle$. Applying (2.4) to the bilinear $\delta X_{\mathbf{q}} \delta X_{-\mathbf{p}-\mathbf{q}}$ yields

$$\langle \delta X_{\mathbf{p}}^M (\delta X_{\mathbf{q}}^I \delta X_{-\mathbf{p}-\mathbf{q}}^J) \rangle_t = \langle \delta X_{\mathbf{p}}^M \delta X_{-\mathbf{p}}^L \rangle_t \frac{\partial \langle \delta X_{\mathbf{q}}^I \delta X_{-\mathbf{q}}^J \rangle'_t}{\partial X^L(t)} \Big|_0 + \dots \quad (2.5)$$

Eq. (2.5) was given by Kenton & Mulryne [38]. The corrections indicated by “ \dots ” include contributions with higher gradients $\sim p^2$ and higher powers of the fluctuation amplitude. Which of these is the leading correction may be model-dependent. In this paper, we do not retain either.

Corrections to Eq. (2.5) from operators containing gradients must involve dimensionless ratios of p with some comparison scale. This ratio determines their relevance. If the background is smooth, the only available scale is the Hubble scale H . The gradient corrections will therefore scale as p/aH . This is typically assumed in the simplest presentations of the “separate universe framework” (to be discussed in more detail in §3), which can also be regarded as an example of an operator product expansion.

Alternatively, if the background is not smooth but contains transitions or other events associated with a particular time t_{event} , and hence a scale $k_{\text{event}} = (aH)_{t=t_{\text{event}}}$, then these scales are also available to form dimensionless ratios. In this case, there may be corrections that scale as powers of p/k_{event} , if the initial time is chosen too early [43]. These effects are described in §3.2. When interpreted within the separate universe framework, demanding that these gradient-dependent terms do not spoil the background evolution is equivalent to the well-known requirement that we should wait for all relevant scales to pass outside the horizon.³ We will see further examples of this requirement in §3. In some cases, the discussion in §3 will show that this constitutes the primary limitation on the utility of separate universe methods to evaluate loop corrections.

3 Loops in the separate universe framework

In addition to the key properties described in §2, we must supply a means to model the time evolution of the perturbations and their correlations. By default, if we wish to accurately model all effects, we should apply a method from non-equilibrium field theory, such as the diagrammatic expansion of the in-in path integral into Green’s functions. Such methods are powerful but technically complex, and it is not always easy to interpret the expressions they produce. As we now explain, under some circumstances the separate universe framework provides an alternative approximate approach. As with any approximation scheme, it has advantages and disadvantages.

3.1 The separate universe framework

The separate universe framework [45–49] is a tool to describe the non-linear evolution of large-scale cosmological perturbations. To use it, we write the number of e-folds accumulated between an initial time t_i and some later time t as $N^{(t_i, t)} \equiv \int_{t_i}^t H(t') dt'$. Now let $\zeta(t)$ denote the curvature perturbation at time t , evaluated in some smoothed patch. In the separate

³For example, this condition was already recognized by Lyth in the early literature on loop corrections; see, Ref. [44], especially the discussion in §III.E.

universe approach, the subsequent evolution of this patch is assumed to follow one of the trajectories of the background phase space. In the simplest scenarios, this trajectory is fixed uniquely by initial conditions set at t_i . The evolution of any perturbed quantity may then be determined by studying how one such patch evolves relative to another. This entails solving its background equations of motion with displaced initial conditions. The leading corrections to this procedure will involve spatial gradients, which (as discussed in §3.2 below) are sometimes, but not always, suppressed on superhorizon scales.

We identify $\zeta(t)$ with the variation δN in the duration of inflation in each patch relative to the mean in a larger volume, now taking t_i to label a spatially-flat initial hypersurface and t to label a uniform-density final hypersurface [45, 46, 50, 51]. We will often regard t as the end of inflation, although this is not required; in principle, t could be any time up to the present, provided it is later than t_i and gradients can be neglected. The initial conditions at t_i are the values of the fields and their momenta.

In principle, this procedure is nonperturbative in the amplitude of each perturbation. In practice, as a matter of convenience, we often invoke an expansion in powers of the initial fluctuation. This yields the well-established “ δN ” Taylor expansion [45, 46, 49]. It provides a description equivalent to cosmological perturbation theory, provided that the time dependence of perturbations with nonzero wavevector \mathbf{k} can be described by the growing and decaying solutions of the homogeneous background. Notice that this does not require the perturbations to be \mathbf{k} -independent, but rather that *any \mathbf{k} -dependence must appear only in the initial amplitude of the growing and decaying modes*.

It does not always happen that each patch follows a single background trajectory. Under certain circumstances, patches may jump stochastically between different available trajectories due to emerging short-scale perturbations. Vennin & Starobinsky described this as the “stochastic δN ” formalism [52, 53]. In this picture, the back-reaction effect we are considering could be interpreted roughly as a single stochastic “kick” near time $t = t_q$, which displaces each patch to a (possibly) different trajectory. However, away from $t = t_q$, the evolution is deterministic.

When it can be applied, the separate universe framework is very appealing. It provides a clear and simple description that accounts for time dependence and the influence of isocurvature modes. The key criterion for applicability is that all \mathbf{k} -dependence is captured in the initial data. There is no guarantee that this is always possible. At a minimum, it requires that the initial time t_i is chosen to be sufficiently late. As we explain below, when back-reaction is neglected, t_i can usually be chosen a little after horizon exit for the \mathbf{k} mode being studied, or after the last transition event of the type to be discussed in §3.2. When back-reaction is included t_i must be chosen later, at least after all modes that back-react have left the horizon. However, we will see that it cannot be chosen too late, otherwise we risk large corrections to the correlation functions at t_i , which would have to be computed using some other method. Although this is possible in principle, much of the simplicity of the separate universe approach would be lost. To avoid this it is necessary to balance a number of effects, and it may not be possible to find an initial hypersurface that satisfies them all; see §3.4. As we discuss below, in this situation it might be necessary to abandon the separate universe framework in favour of an alternative.

3.2 The separate universe framework for models with a non-attractor phase

In §3.3 we use the separate universe method to write down explicit formulae for correlation functions. However, before doing so, we illustrate the necessity of choosing t_i sufficiently late by studying models featuring a transition. Models in which slow-roll evolution is interrupted by an ultra-slow-roll phase (or other non-attractor epoch) belong to this category. A related, complementary discussion has recently been given by Briaud *et al.* [54].

It was explained above that to apply the separate universe framework we must wait until all relevant scales have left the horizon. There is always a *minimum* requirement for all wavenumbers to be in the superhorizon regime, so that gradient corrections scaling as p/aH are small. However, if there are other distinguished events associated with a scale k_{event} , then gradient corrections scaling as p/k_{event} may also enter if t_i is chosen too early.⁴ This issue has recently been emphasized by Jackson *et al.* [43]. In this section we briefly review their analysis. Our main aim is to highlight how gradient data can pass through the calculation to produce $\mathcal{O}(p/k_{\text{event}})$ contributions, even on superhorizon scales, when the background evolution is not smooth.

Superhorizon evolution in slow-roll.—The discussion of §3.1 shows that the (deterministic) separate universe framework requires the future evolution of a smoothed, superhorizon-scale spacetime volume to be uniquely predictable from its initial data.

In this framework we would normally determine perturbations in a field ϕ by solving for the non-perturbative evolution of ϕ with displaced boundary conditions. However, one can also study perturbation equations directly. Here, we follow the second approach. The appropriate equation of motion for a “homogeneous” perturbation (that is, covering an entire smoothed patch) is

$$\frac{d^2\delta\phi_k(\eta)}{d\eta^2} + 2aH \frac{d\delta\phi_k(\eta)}{d\eta} + \left(k^2 + a^2\mathcal{M}\right) \delta\phi_k(\eta) = 0 \quad (3.1)$$

in the limit $k \rightarrow 0$, where η is the conformal time, satisfying $d\eta \equiv dt/a(t)$. The mass \mathcal{M} satisfies

$$\mathcal{M} = V_{\phi\phi} - \frac{1}{a^3} \frac{d}{dt} \left(a^3 \frac{\dot{\phi}^2}{H} \right) = H^2 \times \mathcal{O}(\epsilon), \quad (3.2)$$

where $\mathcal{O}(\epsilon)$ stands for the magnitude of a generic slow-roll parameter. (For definitions, see the beginning of §2.) We caution that the slow-roll parameters cannot be assumed to be always small; e.g., $\epsilon_2 \sim -6$ in ultra-slow-roll inflation.

During a slow-roll epoch, all slow-roll parameters are suppressed and the mass \mathcal{M} can be neglected. The equation of motion is then

$$\frac{d^2\delta\phi_{k \rightarrow 0}(\eta)}{d\eta^2} - \frac{2}{\eta} \frac{d\delta\phi_{k \rightarrow 0}(\eta)}{d\eta} \approx 0, \quad (3.3)$$

whose general solution can be written

$$\delta\phi_{k \rightarrow 0}(\eta) = A + B(-\eta)^3. \quad (3.4)$$

⁴In presentations of the separate universe idea, it is sometimes stated or assumed that gradient corrections always occur in the combination p/aH . As explained here, failure of this property does not itself invalidate the separate universe principle, although it may restrict how it can be applied.

The A -mode is the “growing” mode (here actually a constant), which scales like $(-\eta)^0$. The B -mode is the “decaying” mode, which scales like $(-\eta)^3$. For the separate universe principle to be valid, the time dependence of a perturbation at finite wavevector \mathbf{k} must be a linear combination of these two modes, not necessarily just the “growing” mode. Further, the amplitudes A and B must be predictable from data at the initialization time. Any dependence on \mathbf{k} can be inherited only from the assigned values of A and B .

Let us see how these properties are usually satisfied outside the horizon. Still assuming slow-roll, the \mathbf{k} -dependent solution to Eq. (3.1) is

$$\delta\phi_k(\eta) = \frac{1}{a(\eta)} \left[\alpha \left(1 - \frac{i}{k\eta} \right) e^{-ik\eta} + \beta \left(1 + \frac{i}{k\eta} \right) e^{+ik\eta} \right], \quad (3.5)$$

where α and β are constants encoding the initial data. We typically match to the Bunch–Davies vacuum at past infinity, where $k\eta \rightarrow -\infty$. This gives $\alpha = 1/\sqrt{2k}$ and $\beta = 0$.

Outside the horizon $|k\eta| \sim |k/aH| \ll 1$. Assuming Bunch–Davies initial conditions, and making a Taylor expansion of (3.5) in this limit, yields

$$\delta\phi_k(\eta) \approx \frac{iH}{\sqrt{2}k^{3/2}} \left\{ \textcolor{red}{1} \left[1 + \frac{1}{2}(-k\eta)^2 + \mathcal{O}(-k\eta)^4 \right] + \textcolor{red}{\frac{i}{3}(-k\eta)^3} \left[1 - \frac{1}{10}(-k\eta)^2 + \mathcal{O}(-k\eta)^4 \right] \right\}, \quad (3.6)$$

where we are temporarily taking H to be constant. We recognize the background “growing” and “decaying” modes in red, with time-dependence matching Eq. (3.4). The leading gradient corrections to both “growing” and “decaying” modes are shown in green.

Only the red part of Eq. (3.6) is captured by the separate universe method. The corresponding A - and B -coefficients, as defined in (3.4), are

$$A = \frac{iH}{\sqrt{2}} k^{-3/2}, \quad (3.7a)$$

$$B = \frac{H}{3\sqrt{2}} k^{3/2}. \quad (3.7b)$$

The dominant behaviour as $|k\eta| \rightarrow 0$ comes from the constant “growing” mode. If slow-roll were to continue indefinitely, this solution would give the required evolution outside the horizon.

The leading correction to the separate universe result is of order $(-k\eta)^2$. It comes from the gradient correction to the “growing” mode, not the “decaying” mode. (See also the discussion in Ref. [55].)

Transient non-attractor phase.—Let us now allow a transition to a short non-attractor phase. To be concrete, but without significant loss of generality, we use the example of an ultra-slow-roll phase. We take the transition into ultra-slow-roll to be instantaneous, occurring at cosmic time t_{tr} , or equivalently conformal time η_{tr} . This event defines a distinguished scale, corresponding to k_{event} above, via $k_{\text{tr}} = (aH)_{t_{\text{tr}}}$. Consider a wavevector \mathbf{k} that crosses the horizon just prior to the transition. In this example, the wavenumber k would be located in the region where the power spectrum is growing sharply, like $\mathcal{P}_\zeta(k) \propto k^4$. The solution up to η_{tr} is given by (3.6). Up to and including the first contribution from the “decaying” mode,

it is

$$\delta\phi_{\mathbf{k}}^{\text{SR}}(\eta) = \frac{iH\alpha}{k} \left(1 + \frac{1}{2}(-k\eta)^2 + \frac{i}{3}(-k\eta)^3 \right) + \mathcal{O}(-k\eta)^4 \quad \text{if } \eta < \eta_{\text{tr}}. \quad (3.8)$$

As is now well-known, during ultra-slow-roll, the mass term (3.2) turns out to have the same value as in slow-roll, even though $\epsilon_2 \sim -6$. (This is an example of *Wands duality* [56].) Therefore the solution to the $\delta\phi$ mode equation will be the same as (3.5), but with differing coefficients α, β . Labelling these with a tilde, viz. $\tilde{\alpha}, \tilde{\beta}$, we have

$$\delta\phi_{\mathbf{k}}^{\text{USR}}(\eta) = \frac{iH}{k}(\tilde{\alpha} - \tilde{\beta}) \left(1 + \frac{1}{2}(-k\eta)^2 \right) - \frac{H}{3k}(\tilde{\alpha} + \tilde{\beta})(-k\eta)^3 + \mathcal{O}(-k\eta)^4 \quad \text{if } \eta > \eta_{\text{tr}}. \quad (3.9)$$

To determine $\tilde{\alpha}, \tilde{\beta}$, we require matching conditions at η_{tr} . The required conditions are⁵

$$\delta\phi_{\mathbf{k}}^{\text{USR}} \Big|_{\eta=\eta_{\text{tr}}} = \delta\phi_{\mathbf{k}}^{\text{SR}} \Big|_{\eta=\eta_{\text{tr}}} \quad (3.11a)$$

$$\frac{d\delta\phi_{\mathbf{k}}^{\text{USR}}}{d\eta} \Big|_{\eta=\eta_{\text{tr}}} = \left(\frac{d\delta\phi_{\mathbf{k}}^{\text{SR}}}{d\eta} - 3k_{\text{tr}}\delta\phi_{\mathbf{k}}^{\text{SR}} \right) \Big|_{\eta=\eta_{\text{tr}}}. \quad (3.11b)$$

The jump in the derivative, enforced by Eq. (3.11b), is responsible for the difference between α, β and $\tilde{\alpha}, \tilde{\beta}$. Solving for $\tilde{\alpha}, \tilde{\beta}$ and inserting these into (3.9), we find

$$\delta\phi_{\mathbf{k}}^{\text{USR}}(\eta) = \frac{iH}{\sqrt{2}k^{3/2}} \left\{ \left[-\frac{2}{5} \left(\frac{k}{k_{\text{tr}}} \right)^2 + \mathcal{O} \left(\frac{k}{k_{\text{tr}}} \right)^3 \right] \left(\textcolor{red}{1} + \frac{1}{2}(-k\eta)^2 + \mathcal{O}(-k\eta)^4 \right) + \left[\left(\frac{k}{k_{\text{tr}}} \right)^{-3} + \mathcal{O} \left(\frac{k}{k_{\text{tr}}} \right)^{-1} \right] \left((-k\eta)^3 + \mathcal{O}(-k\eta)^5 \right) \right\}, \quad (3.12)$$

where k_{tr} labels the horizon scale at the transition time, i.e. $k_{\text{tr}}/aH \approx 1$ at $\eta = \eta_{\text{tr}}$. As before, we have highlighted the lowest-order ‘‘growing’’ and ‘‘decaying’’ modes in **red**, and the leading gradient correction in **green**. Note that Eq. (3.12) is well-behaved as $k \rightarrow 0$, despite the appearance of inverse powers of k/k_{tr} in $\tilde{\alpha} + \tilde{\beta}$.

The corresponding separate universe A - and B -coefficients are

$$A \approx -\frac{2iH}{5\sqrt{2}} \left(\frac{k}{k_{\text{tr}}} \right)^2 k^{-3/2}, \quad (3.13a)$$

$$B \approx -\frac{iH}{\sqrt{2}} \left(\frac{k}{k_{\text{tr}}} \right)^{-3} k^{3/2}. \quad (3.13b)$$

⁵Notice that while $\delta\phi_{\mathbf{k}}(\eta)$ is continuous at the transition, its derivative is not. The matching condition can be obtained by modelling the slow-roll to ultra-slow-roll transition using Starobinsky’s piece-wise linear model [57]. This yields

$$\frac{d\delta\phi_{\mathbf{k}}^{\text{USR}}}{d\eta} \Big|_{\eta=\eta_{\text{tr}}} = \left(\frac{d\delta\phi_{\mathbf{k}}^{\text{SR}}}{d\eta} + 3\frac{\Delta A}{A_+} k_{\text{tr}}\delta\phi_{\mathbf{k}}^{\text{SR}} \right) \Big|_{\eta=\eta_{\text{tr}}}, \quad (3.10)$$

where $A_+ > 0$ ($A_- > 0$) is the slope of the potential before (after) the transition, and $\Delta A \equiv A_- - A_+$. Ultra-slow-roll is realized when $A_- \ll A_+$. In this limit, Eq. (3.10) matches the second condition given in Eq. (3.11b).

For a long-wavelength mode that did not cross much before the transition, k/k_{tr} will not be too much smaller than unity.⁶ At least a few e-folds after the transition, we also have $|k_{\text{tr}}\eta| \ll 1$, so both the ‘‘decaying’’ mode and the gradient correction to the ‘‘growing’’ mode can be dropped. In the power spectrum, it follows that the A -coefficient for the ‘‘growing’’ mode will yield the expected growing behaviour $\mathcal{P}_\zeta \propto k^4$.

Eq. (3.12) satisfies the separate universe principle at times later than the transition. It yields A and B coefficients that do not agree with the pre-transition solution (3.8), which clearly is to be expected. The critical feature of (3.12)–(3.13a) is not the difference as such, but rather that the $(k/k_{\text{tr}})^2$ scaling of the A -coefficient in (3.13a) cannot be reproduced by the $k \rightarrow 0$ limit of (3.1) with initial condition (3.7a). A similar statement applies to the B coefficient. The appearance of k/k_{tr} is attributable to imposition of the jump condition (3.11b) at a localized time η_{tr} . In other words, it follows from the presence of a sudden transition in the background.

The conclusion is that the separate universe framework correctly describes the time dependence of the perturbation for each \mathbf{k} -mode, but only if we use initial data determined *after* the transition. In the language of §3.1, this ensures that the subsequent evolution of each superhorizon volume is uniquely predictable from its initial conditions. This conclusion was emphasized by Ref. [43]. Although not shown here, the choice $t_i > t_{\text{tr}}$ actually allows a correct description of all large scales, not just those that exit not too long before the transition. In Appendix A we show that, for two independent choices of initial time $t_i > t_{\text{tr}}$, the separate universe principle successfully reproduces the numerical tree-level power spectrum for the toy model considered in Ref. [2].

3.3 Correlation functions

With these considerations in mind, we now explain how to compute correlation functions in the scenario of §2, where there is a back-reaction event at some time t_q .

Tree-level δN formula in phase space.—To begin, we work at tree level. We choose an initial time t_i just after some large-scale mode \mathbf{p} has left the horizon, and smooth on the scale $L \sim p^{-1}$. As explained above, each resulting patch evolves like a locally unperturbed universe with displaced initial conditions. Making a δN Taylor expansion in these displacements, and dropping gradients, we find that the change δX^I from patch to patch in some field X^I is

$$[\delta X^I(t, \mathbf{x})]_L = \frac{\partial X^I(t)}{\partial X^M(t_i)} [\delta X^M(t_i, \mathbf{x})]_L + \frac{1}{2!} \frac{\partial^2 X^I(t)}{\partial X^M(t_i) \partial X^N(t_i)} [\delta X^M(t_i, \mathbf{x})]_L [\delta X^N(t_i, \mathbf{x})]_L \\ + \frac{1}{3!} \frac{\partial^3 X^I(t)}{\partial X^M(t_i) \partial X^N(t_i) \partial X^R(t_i)} [\delta X^M(t_i, \mathbf{x})]_L [\delta X^N(t_i, \mathbf{x})]_L [\delta X^R(t_i, \mathbf{x})]_L + \dots, \quad (3.14)$$

where $[\dots]_L$ denotes smoothing on the scale L . The smoothing implies that the spatial coordinate \mathbf{x} should be regarded as labelling each patch. The notation $\partial X^I(t)/\partial X^M(t_i)$

⁶Our aim here is only to illustrate the effect of gradient terms in models with a transition, and discuss the correct choice of initialization time. For this reason, we restrict our attention to modes that crossed the horizon just before the transition. In order to model the behaviour of substantially larger scales, such as CMB scales, or the scale corresponding to the dip in \mathcal{P}_ζ , one would need to keep track of all factors (e.g. $\Delta A \neq -A_+$ in Eq. (3.10)), as done in Ref. [43].

(and its higher-order generalizations) denotes the variation of a late-time field $X^I(t)$ with respect to a displacement in the early-time initial condition $X^M(t_i)$. Eq. (3.14) enables us to determine correlation functions of the perturbation $[\delta X(t)]_L$ at wavevector \mathbf{p} , at any time up to the point where enhanced small-scale modes emerge. This is analogous to the transition time t_{tr} from §3.2. For convenience, we continue to label this time t_q , with the understanding that all back-reacting modes should have exited the horizon by that time. Eq. (3.14) is invalidated once back-reaction becomes important, because the fields are no longer determined only by initial data at t_i . This parallels the difference between the pre- and post-transition solutions (3.7a) and (3.13a).

To build correlation functions from (3.14), we use it to define Fourier modes and evaluate suitable expectation values. When we do so, we encounter many possible terms. These can be classified according to the number of unconstrained momentum integrals they contain. ‘Tree-level’ contributions contain no unconstrained momentum integrals. We may also encounter ‘loop-level’ terms. By analogy with quantum field theory, a term is said to be at n^{th} order in the loop expansion when it contains n unconstrained integrals. Smoothing on the scale $L \sim p^{-1}$ implies that these integrals will effectively be cut off for comoving momenta $\gtrsim p$. The tree-level expression, Eq. (3.14), has no knowledge of the short-scale modes. It therefore neglects any back-reaction.

At this stage, the notion of ‘loop-level’ used here is simply a formal definition and does not imply any relationship with loops generated by the expansion of “in–in” quantum field theory into Green’s functions.

δN formula with back-reaction.—To capture back-reaction we make two changes. First, Eq. (3.12) shows that when back-reaction modifies the background we must choose new initial data, to capture effects involving powers of p/q . This ratio is analogous to k/k_{tr} . We are therefore forced to move the initial time t_i to be later than t_q . Second, we must calculate the relevant (p/q) -corrected effects. To do so, we introduce averages over the short-scale modes by working beyond tree-level in the loop expansion. This procedure was described in Ref. [2], and we briefly summarize the steps below. Up to limitations set by our approximations, it is valid provided $p/q \ll 1$, so that there is an appreciable separation of scales.

We continue to label the new initial hypersurface with time label t_i . It must be chosen late enough to allow horizon exit for all modes that contribute to the back-reaction. We populate this hypersurface with smoothed horizon volumes of size ℓ . Separation of scales means that ℓ is much smaller than the initial smoothing scale L . The distribution of Fourier modes in these volumes includes contributions from all scales that exited the horizon between (at least) t_p and t_q . Applying Eq. (3.14), now specialized to the curvature perturbation ζ , and extracting a long-wavelength Fourier wavevector \mathbf{p} , we obtain

$$\begin{aligned} \zeta_{\mathbf{p}}(t) = & N_I^{(t_i,t)} \left[[\delta X^I(t_i, \mathbf{x})]_L \right]_{\mathbf{p}} + \frac{1}{2!} N_{IJ}^{(t_i,t)} \int \frac{d^3 r}{(2\pi)^3} \left[[\delta X^I(t_i, \mathbf{x})]_L \right]_{\mathbf{p}-\mathbf{r}} \left[[\delta X^J(t_i, \mathbf{x})]_L \right]_{\mathbf{r}} \\ & + \frac{1}{3!} N_{IJK}^{(t_i,t)} \int \frac{d^3 r}{(2\pi)^3} \frac{d^3 s}{(2\pi)^3} \left[[\delta X^I(t_i, \mathbf{x})]_L \right]_{\mathbf{p}-\mathbf{r}-\mathbf{s}} \left[[\delta X^J(t_i, \mathbf{x})]_L \right]_{\mathbf{r}} \left[[\delta X^K(t_i, \mathbf{x})]_L \right]_{\mathbf{s}} \\ & + \mathcal{O}(\delta X)^4. \end{aligned} \quad (3.15)$$

Each integral should now be cut off for wavenumbers $\gtrsim \ell^{-1}$. The notation $[[\delta X^I]_{\text{e}}]_{\mathbf{p}}$ indicates that we *first* smooth on the scale ℓ , and *then* extract the Fourier mode \mathbf{p} . This smoothing procedure may already disturb the \mathbf{p} -mode of δX^I , when compared to the value that would be predicted by (3.14). This corresponds to the possibility of a non-negligible loop correction to δX^I at time t_i . We discuss this in more detail in §5.

1-loop contributions.—Eq. (3.15) yields four contributions to the 2-point function $\langle \zeta_{\mathbf{p}}(t) \zeta_{-\mathbf{p}}(t) \rangle'$. These are

$$\langle \zeta_{\mathbf{p}}(t) \zeta_{-\mathbf{p}}(t) \rangle'_{\text{1-loop}} = \underbrace{\langle \zeta_{\mathbf{p}} \zeta_{-\mathbf{p}} \rangle'_{11}}_{\substack{\text{1-loop in} \\ \text{initial conditions}}} + \underbrace{\langle \zeta_{\mathbf{p}} \zeta_{-\mathbf{p}} \rangle'_{12} + \langle \zeta_{\mathbf{p}} \zeta_{-\mathbf{p}} \rangle'_{22} + \langle \zeta_{\mathbf{p}} \zeta_{-\mathbf{p}} \rangle'_{13}}_{\text{1-loop due to non-linearity of } \delta N}, \quad (3.16)$$

where we have labelled each piece based on the contributions from Eq. (3.15); “1” labels the linear term, “2” the quadratic term, and “3” the cubic term. Explicitly, these can be written

$$\langle \zeta_{\mathbf{p}} \zeta_{-\mathbf{p}} \rangle'_{11} = N_I^{(t_i, t)} N_J^{(t_i, t)} \left\langle \left[[\delta X^I(t_i, \mathbf{x})]_{\text{e}} \right]_{\mathbf{p}} \left[[\delta X^J(t_i, \mathbf{x})]_{\text{e}} \right]_{-\mathbf{p}} \right\rangle'_{\text{1-loop}}, \quad (3.17a)$$

$$\begin{aligned} \langle \zeta_{\mathbf{p}} \zeta_{-\mathbf{p}} \rangle'_{12} &= \frac{1}{2} N_I^{(t_i, t)} N_{JK}^{(t_i, t)} \int \frac{d^3 r}{(2\pi)^3} \left(\left\langle \delta X_{\mathbf{p}}^I(t_i) \delta X_{\mathbf{r}}^J(t_i) \delta X_{-\mathbf{p}-\mathbf{r}}^K(t_i) \right\rangle'_{\text{tree}} \right. \\ &\quad \left. + \left\langle \delta X_{\mathbf{r}}^J(t_i) \delta X_{\mathbf{p}-\mathbf{r}}^K(t_i) \delta X_{-\mathbf{p}}^I(t_i) \right\rangle'_{\text{tree}} \right), \end{aligned} \quad (3.17b)$$

$$\langle \zeta_{\mathbf{p}} \zeta_{-\mathbf{p}} \rangle'_{22} = \frac{1}{4} N_{IJ}^{(t_i, t)} N_{KM}^{(t_i, t)} \int \frac{d^3 r}{(2\pi)^3} \frac{d^3 s}{(2\pi)^3} \left\langle \delta X_{\mathbf{r}}^I(t_i) \delta X_{\mathbf{p}-\mathbf{r}}^J(t_i) \delta X_{\mathbf{s}}^K(t_i) \delta X_{-\mathbf{p}-\mathbf{s}}^M(t_i) \right\rangle'_{\text{tree}}, \quad (3.17c)$$

$$\begin{aligned} \langle \zeta_{\mathbf{p}} \zeta_{-\mathbf{p}} \rangle'_{13} &= \frac{1}{6} N_I^{(t_i, t)} N_{JKM}^{(t_i, t)} \int \frac{d^3 r}{(2\pi)^3} \frac{d^3 s}{(2\pi)^3} \left(\left\langle \delta X_{\mathbf{p}}^I(t_i) \delta X_{\mathbf{r}}^J(t_i) \delta X_{\mathbf{s}}^K(t_i) \delta X_{-\mathbf{p}-\mathbf{r}-\mathbf{s}}^M(t_i) \right\rangle'_{\text{tree}} \right. \\ &\quad \left. + \left\langle \delta X_{\mathbf{r}}^J(t_i) \delta X_{\mathbf{s}}^K(t_i) \delta X_{\mathbf{p}-\mathbf{r}-\mathbf{s}}^M(t_i) \delta X_{-\mathbf{p}}^I(t_i) \right\rangle'_{\text{tree}} \right). \end{aligned} \quad (3.17d)$$

At this order in the loop expansion, only the 11-type contribution includes a loop correction to the initial δX correlation functions. Such corrections can be ignored in the remaining contributions. We have therefore approximated $[[\delta X^I]_{\text{e}}]_{\mathbf{k}} \approx \delta X_{\mathbf{k}}^I$. In what follows, we distinguish between the two types of contribution in Eq. (3.16) by describing the (12)-, (22)- and (13)-type loops as “ δN loops” [58].

3.4 Does the separate universe framework capture “in–in” loop effects?

In the language of §3.2, the time-dependent separate-universe factors $N_I^{(t_i, t)}$, $N_{IJ}^{(t_i, t)}$ and $N_{IJK}^{(t_i, t)}$ in Eqs. (3.17a)–(3.17d) contain the red-highlighted time-dependent growing and decaying modes in (3.12). Meanwhile, the δX^I correlation functions determine the initial data. They correspond to (expectation values of) the \mathbf{k} -dependent A - and B -coefficients of Eqs. (3.13a)–(3.13b). In the full theory A and B are stochastic variables, which inherit their stochasticity from the initial data at time t_p . The loop integrals average over the short-scale modes, and measure their influence on the evolution of the large-scale mode \mathbf{p} . Dependence on p/q

arises from these integrals and from the δX^I correlation functions. It follows that loop-level formulae such as (3.17a)–(3.17d) can be regarded as an approximation that captures some features of back-reaction. As usual, whether this approximation is adequate for any particular purpose depends on the model being studied and the observable under discussion.

We have already emphasized that, as presented here, separate-universe loop-level expressions such as Eqs. (3.17a)–(3.17d) do not yet have a clear relationship with the loop expansion of non-equilibrium quantum field theory, represented by (for example) the loop expansion of the “in–in” path integral. In Ref. [2] it was assumed, but not demonstrated, that the “separate-universe” loops of Eq. (3.17a)–(3.17d) represented a subset of the “in–in” loops, so that it was meaningful to compare calculations performed in these different frameworks. For example, if the enhanced modes contributing to these integrals are on superhorizon scales, and behaving nearly classically, one would expect that their contribution could be captured in either formalism.

This expectation can be made more precise. A comprehensive explanation of the relation between the separate universe framework and “in–in” perturbation theory requires more elaboration than can be given here, and we will return to it in a separate publication [59]. Here, we simply summarize the key ideas. Starting from either the operator Heisenberg equation of motion, or an explicit 1-loop formula for the correlation function, it is possible to derive a 1-loop transport equation for the two-point function. Working in a compact de Witt notation, where index summation implies integration over \mathbf{k} labels (for details, see, e.g., Ref. [60]), this equation can be written, for generic fields X^I ,

$$\begin{aligned} \frac{d}{dN} \langle X^I X^J \rangle &= u^I_M \langle X^M X^J \rangle + u^J_M \langle X^I X^M \rangle \\ &\quad + \frac{1}{2} u^I_{MN} \langle X^M X^N X^J \rangle + \frac{1}{2} u^J_{MN} \langle X^I X^M X^N \rangle \\ &\quad + \frac{1}{2} u^I_{MNR} \langle X^M X^J \rangle \langle X^N X^R \rangle + \frac{1}{2} u^J_{MNR} \langle X^I X^M \rangle \langle X^N X^R \rangle. \end{aligned} \quad (3.18)$$

The tensors u^I_M , u^I_{MN} , u^I_{MNR} depend on the background trajectory, and the wavenumbers carried by their indices. Explicit expressions for u^I_M and u^I_{MN} were given in Dias *et al.* [60], valid for the case that the X^I are perturbations in the fields and momenta on a spatially flat slicing. The zero-wavenumber limit of u^I_{MNR} was obtained by Andersen *et al.* [61]. An exact wavenumber-dependent expression for it is not yet known, but is not needed at the level of the present discussion. Eq. (3.18) should be supplemented by a tree-level transport equation for the 3-point function, described in Ref. [60]. This system of coupled transport equations for the 2- and 3-point functions can be integrated by writing

$$(X^I)_t = \Gamma^I_M (X^M)_{t^*} + \frac{1}{2!} \Gamma^I_{MN} (X^M X^N)_{t^*} + \frac{1}{3!} \Gamma^I_{MNR} (X^M X^N X^R)_{t^*} + \dots, \quad (3.19)$$

where $t^* < t$, and $(\dots)_t$ denotes evaluation of the enclosed operator at time t . Eq. (3.19) can be regarded as a form of operator product expansion, in which the operator $(X^I)_t$ is interpreted as composite with respect to a basis of operators defined at t^* . The Γ -tensors play the role of OPE coefficients. For convenience we assume the operators $(X^M X^N)_{t^*}$, $(X^M X^N X^R)_{t^*}$ to be symmetrized.

The momentum-dependent tensors (technically bitensors) $\Gamma^I{}_M$, $\Gamma^I{}_{MN}$, $\Gamma^I{}_{MNR}$ satisfy evolution equations that symbolically match those already known at tree-level, although now with momentum-dependent u -tensors. For the $\Gamma^I{}_M$ tensor the required equation is [62, 63]

$$\frac{d}{dN} \Gamma^I{}_M = u^I{}_J \Gamma^J{}_M. \quad (3.20)$$

Corresponding equations for the $\Gamma^I{}_{MN}$ and $\Gamma^I{}_{MNR}$ tensors can be found in Dias *et al.* [60] and Anderson *et al.* [61]. The initial conditions require $\Gamma^I{}_M = \delta^I{}_M$ at $t = t^*$, with all other Γ -tensors equal to zero. We discuss the Γ -tensors in more detail in §5.

We can now connect this picture with the separate universe framework. The initial time t^* appearing in Eq. (3.19) is arbitrary, because it merely corresponds to breaking the integration of (3.18) into two steps: an integral up to t^* , followed by an integral from t^* to t . As a result, Eq. (3.19) solves the transport equation in the sense that the 2-point function computed using it matches direct solution of Eq. (3.18), provided correlations of the operators on the right-hand side of (3.19) are computed using the same system of transport equations, or equivalently, to 1-loop for 2-point functions and tree-level for 3-point functions. However we choose t^* , the result matches the 1-loop “in–in” expression (before imposing a cutoff) provided all momentum-dependent effects are retained in the Γ -tensors and the X^I correlation functions at t^* .

We now choose t^* to match the initial time t_i used in Eqs. (3.17a)–(3.17d). The u -tensors $u^I{}_M$, $u^I{}_{MN}$ and $u^I{}_{MNR}$ have local expressions and may depend on $p/(aH)$ and $q/(aH)$, but not on the ratio q/p .⁷ The same dependences will be inherited by the Γ -tensors. With initial conditions set after all back-reacting modes leave the horizon, their values will therefore be close to those predicted by the separate universe framework because integration of the Γ -tensors in the zero-momentum limit is known to reproduce the Taylor expansion in initial conditions [62]. At 1-loop order, this includes a slight shift in $u^I{}_M$ corresponding to a tadpole. After making a gauge transformation to ζ , the result is that Eq. (3.19) will lead to a set of 1-loop expressions equivalent to Eqs. (3.17a)–(3.17d), up to corrections of order $p/(aH)$ and $q/(aH)$. As we have already emphasized, the initial correlation functions appearing in Eqs. (3.17a)–(3.17d) must include loop corrections to the 11 initial condition, evaluated up to time t_i .

These loop integrals clearly will **not** capture contributions to the full “in–in” loops from regions of the momentum integration where $q/aH \gtrsim 1$. This is not only expected but guaranteed, because the separate universe method does not accurately capture effects occurring on subhorizon scales. However, for the problem at hand we wish only to capture effects from the band of enhanced short-scale modes, which at this stage have been inflated to superhorizon scales. In this region, as we have seen, the Γ -tensors are nearly independent of wavenumber and closely approximate the values predicted by the separate universe framework. Contributions to the complete “in–in” loop integrals from back-reacting modes on

⁷This can be demonstrated explicitly for $u^I{}_M$ and $u^I{}_{MN}$, for which complete momentum-dependent expressions are known; see Ref. [60]. The formulae quoted there for $u^I{}_{MN}$ appear non-local, but this can be removed using the Hamiltonian constraint, as discussed in Dias *et al.* [64]. One expects this property to apply at all orders. It must be true for $u^I{}_{MNR}$ in order to smoothly connect with the zero-momentum expressions quoted by Anderson *et al.* [61].

superhorizon scales should therefore be captured equally well using either method. Provided the final renormalization scale is reasonably larger than the ultraviolet end of the enhanced band, we expect this conclusion will not be significantly altered by ultraviolet regularization and renormalization.

Use of the separate universe formulae (3.17a)–(3.17d) has a number of advantages compared to the full “in–in” calculation. These expressions are substantially less complex than those produced by an expansion of “in–in” diagrams into Green’s functions. As a result, the physical mechanism of back-reaction is more explicit. Further, it is much easier to include the effect of multiple scalar fields, and to track time dependence accurately outside the horizon.

Choice of initial time.— The main drawback with the programme outlined above is the necessity of including loop corrections to the initial condition. Its 1-loop correction represents disturbance of the long \mathbf{p} mode by short-scale structure even before the initial time t_i , as already pointed out below Eq. (3.17d). This implies that we must balance competing requirements when choosing the initial time t_i .

We have seen that the δN loops of Eqs. (3.17b)–(3.17d) provide an accurate estimate for loop momenta in the enhanced band only if t_i is chosen after all back-reacting scales exit the horizon. In fact, if the peak is produced by modes enhanced during an ultra-slow-roll phase, modes exiting after a later return to slow-roll may also contribute to the broad peak in the power spectrum. To capture the effect of all these modes it may be necessary to choose t_i *substantially* later than the time of the transition. We will comment on the inclusion of the whole peak in §4.2.

On the other hand, the later we choose t_i , the more significant loop corrections to the initial correlation function in (3.17a) are likely to become. Such corrections are not expected to be large during slow-roll evolution [65], but it is plausible that there could be a significant effect in the ultra-slow-roll epoch. To make our application of the separate universe method as simple as possible, the initial time should be set sufficiently *early* that the initial correlations are affected minimally by such effects.⁸ Clearly, these desiderata are in some tension, and it may not be possible to find a t_i that satisfies all of these requirements.

3.5 The 1-loop contributions

For future convenience, we collect reduced expressions for the contribution to the power spectrum from the (11)-, (12)-, (22)-, and (13)-type loops, given by Eqs. (3.17a)–(3.17d).

Note that we do not need to account for further loop contributions. In particular, the initial correlation functions absorb all loop corrections up to the initial time t_i . The separate universe contributions (such as Eqs. (3.17b)–(3.17d) at 1-loop) absorb corrections generated between t_i and the time of observation, t . This includes all loop corrections generated by nonlinear evolution of the underlying fields and momenta X^I , *and* nonlinearities associated

⁸We emphasize that this is not an issue of principle, but only convenience. If it is not possible to choose t_i early enough that the δX^I are not contaminated by loop corrections, one could always choose to evaluate them using the in–in formalism or an equivalent. However, in this case, the simplicity of the separate universe method is largely lost. Whatever method we choose to evaluate the loop corrections to the δX^I , we might as well calculate the entire loop correction to ζ in the same way.

with the gauge transformation into ζ . The δN formula accounts for all these sources of nonlinearity, not merely those associated with the gauge transformation to ζ .

(11)-type loop.—The (11)-type loop is given by Eq. (3.17a). We can write it in the more economical form

$$\langle \zeta_{\mathbf{p}}(t) \zeta_{-\mathbf{p}}(t) \rangle'_{11} = N_I^{(t_i,t)} N_J^{(t_i,t)} \langle \delta X_{\mathbf{p}}^I(t_i) \delta X_{-\mathbf{p}}^J(t_i) \rangle'_{1\text{-loop}}, \quad (3.21)$$

in which the explicit smoothing has been dropped. As explained above, this is replaced by the 1-loop correction.

(12)-, (22)-, and (13)-type loops.—The (12)-, (22)- and (13)-type diagrams are associated with non-linear terms in the δN formula (3.15), which induce correlations between the long- and short-scale modes. The primary expressions are Eqs. (3.17b)–(3.17d). Below, the loop momentum variable (\mathbf{r} or \mathbf{s} in Eqs. (3.17b)–(3.17d)) has been relabelled \mathbf{q} .

The expressions for these terms can be simplified in our assumed momentum configuration, where there is a large hierarchy $p \ll q$. In this configuration, the operators $\delta \hat{X}_{\mathbf{p}}^I$ and $\delta \hat{X}_{\mathbf{q}}^J$ commute. Also, the 3-point correlation function (1.4b) depends only on the magnitude of the momenta. Dropping corrections of relative order $(p/q)^2$, so that we can write $|\mathbf{p} + \mathbf{q}| \approx q$, it follows that the (12)-type loop (3.17b) can be written

$$P_{\zeta}(p; t)_{12} = N_I^{(t_i,t)} N_{JK}^{(t_i,t)} \int d^3 q \alpha^{IJK}(p, q, q; t_i). \quad (3.22)$$

Making the same approximations, the (22)-type diagram (3.17c) reduces to

$$P_{\zeta}(p; t)_{22} = \frac{1}{2} N_{IJ}^{(t_i,t)} N_{KL}^{(t_i,t)} \int d^3 q P^{IK}(q; t_i) P^{JL}(q; t_i). \quad (3.23)$$

Finally, after performing Wick contractions in Eq. (3.17d) we find that the (13)-contribution can be rewritten

$$P_{\zeta}(p; t)_{13} = \frac{1}{2} N_I^{(t_i,t)} N_{JKL}^{(t_i,t)} [P^{IJ}(p; t_i) + P^{JI}(p; t_i)] \int d^3 q P^{KL}(q; t_i). \quad (3.24)$$

During inflation, the commutator of the field operator and its momentum decays rapidly after horizon crossing,

$$[\delta \hat{\phi}_{\mathbf{k}}(t), \delta \hat{\pi}_{\mathbf{k}'}(t')] = i(2\pi)^3 \delta(\mathbf{k} + \mathbf{k}') \delta(t - t') a(t)^{-2}. \quad (3.25)$$

Since the initial time t_i will typically be much later than the horizon exit time t_p for \mathbf{p} , we can take operators associated with the long mode to commute at time t_i . It follows that the power spectrum $P^{IJ}(p; t_i)$ will be symmetric. Hence, we find

$$P_{\zeta}(p; t)_{13} = N_I^{(t_i,t)} N_{JKL}^{(t_i,t)} P^{IJ}(p; t_i) \int d^3 q P^{KL}(q; t_i). \quad (3.26)$$

The (22)-type loop can be regarded as an average over uncorrelated noise on the scale q^{-1} [2]. When averaged over a spacetime region of size p^{-1} we obtain $\mathcal{N} \sim (q/p)^3$ independent samples of this noise. If they are uncorrelated, the central limit theorem implies that the variance of their average is suppressed by $1/\mathcal{N} \sim (p/q)^3$. In the literature, this is described as *volume*

suppression. Meanwhile, the (12)- and (13)-type loops (3.17b) and (3.17d) incorporate long–short couplings, in the form of initial conditions on squeezed configurations. As explained in Ref. [2], these correlations invalidate a naïve application of the central limit theorem. The result is that the (12)- and (13)-type loops need not exhibit the same volume suppression.

In the remainder of this paper, we discard the (22)-type diagram and focus on the (12)- and (13)-type contributions.

4 1-loop from non-linear superhorizon evolution is a boundary term

In §4.1 we will derive one of our main results. Starting from the δN formula (3.15) for the long-wavelength mode, we show that the (12)- and (13)-type loops can be unified into a single loop integral. The integrand is a total derivative of a function we are able to identify explicitly. We elaborate on the interpretation of our result in §4.2.

4.1 Combining the (12)- and (13)-type loops

From Eqs. (3.22) and (3.26), the sum of the (12)- and (13)-type loops is

$$P_\zeta(p; t)_{12+13} = N_I^{(t_i, t)} N_{JK}^{(t_i, t)} \int d^3 q \alpha^{IJK}(p, q, q; t_i) + N_I^{(t_i, t)} N_{JKL}^{(t_i, t)} \int d^3 q P^{IJ}(p; t_i) P^{KL}(q; t_i). \quad (4.1)$$

The squeezed bispectrum $\alpha^{IJK}(p, q, q; t_i)$ can be estimated by soft-limit arguments [37–39]; see §2. At leading order in $p \ll q$, Eq. (2.5) and the definition (1.4b) yield⁹

$$\alpha^{IJK}(p, q, q; t_i) \supseteq P^{IL}(p; t_i) \frac{\partial P^{JK}(q; t_i)}{\partial X^L(t_i)}. \quad (4.2)$$

Substitution of Eq. (4.2) in Eq. (4.1) yields

$$P_\zeta(p; t)_{12+13} = N_I^{(t_i, t)} P^{IL}(p; t_i) \int d^3 q \left[N_{JK}^{(t_i, t)} \frac{\partial P^{JK}(q; t_i)}{\partial X^L(t_i)} + N_{LJK}^{(t_i, t)} P^{JK}(q; t_i) \right], \quad (4.3)$$

where we have relabelled summation indices in the second term. Note that the δN coefficients N_J , N_{JK} , and N_{LJK} have no momentum dependence; they carry information only about the background evolution, and therefore commute with the integral. By rearranging the derivatives we obtain

$$P_\zeta(p; t)_{12+13} = N_I^{(t_i, t)} \int d^3 q P^{IL}(p; t_i) \frac{\partial}{\partial X^L(t_i)} \left[N_{JK}^{(t_i, t)} P^{JK}(q; t_i) \right]. \quad (4.4)$$

On the other hand, the derivative $\partial/\partial X^L(t_i)$ with respect to the initial conditions at t_i does *not* commute with the integral, even though the notation suggests that it is momentum independent. This is because, under a shift in its initial data, the change in the quantity enclosed by square brackets $[\dots]$ can be q -dependent even if the shift in $X^L(t_i)$ is not. The

⁹The rationale for Eq. (4.2) is fairly clear at horizon exit of q . One might be concerned that evolution between this time and t_i could change the relationship, but in Appendix B we show this is not the case.

fact the 1-loop correction can be organized in this form shows clearly that it measures the correlation between the response of the short scale modes to the long mode, and the original long mode. Moreover, the response of the short modes is expressed in terms of a shift in their effective background. This is a consequence of our assumed separation of scales, so that modes in the enhanced band have $q \gg p$.

The shift of $X^L(t_i)$ does not change the numerical value of q , so we may freely move a factor q^{-3} past the derivative. This exchanges the short-scale power spectrum $P^{JK}(q)$ for its dimensionless counterpart $\mathcal{P}^{JK}(q)$,

$$P_\zeta(p; t)_{12+13} = N_I^{(t_i, t)} \int d \ln q \, P^{IL}(p; t_i) \frac{\partial}{\partial X^L(t_i)} \left[N_{JK}^{(t_i, t)} \mathcal{P}^{JK}(q; t_i) \right]. \quad (4.5)$$

In what follows, we give a concrete calculation by specializing to a single-field scenario in which the phase-space indices I, J, \dots , run over the coordinates $\{\phi, \pi\}$. We expect effectively the same analysis to apply whenever the field configuration for the mode \mathbf{p} is adiabatic, but we leave an explicit demonstration for future work.

Writing out the sum over L explicitly yields

$$P_\zeta(p; t)_{12+13} = N_I^{(t_i, t)} \int d \ln q \left(P^{I\phi}(p; t_i) \frac{\partial}{\partial \phi(t_i)} + P^{I\pi}(p; t_i) \frac{\partial}{\partial \pi(t_i)} \right) \left[N_{JK}^{(t_i, t)} \mathcal{P}^{JK}(q; t_i) \right]. \quad (4.6)$$

The assumption of adiabaticity means that fluctuations in the field and its momentum are not independent. Using Eqs. (2.1) and (4.6) allows us to write

$$P_\zeta(p; t)_{12+13} = N_I^{(t_i, t)} \int d \ln q \, P^{I\phi}(p; t_i) \left(\frac{\partial}{\partial \phi(t_i)} + \frac{\epsilon_2}{2} \frac{\partial}{\partial \pi(t_i)} \right) \left[N_{JK}^{(t_i, t)} \mathcal{P}^{JK}(q; t_i) \right]. \quad (4.7)$$

This combination of partial derivatives is merely the total derivative with respect to ϕ , evaluated along the unperturbed trajectory; see Eq. (2.2). Therefore,

$$\mathcal{P}_\zeta(p; t)_{12+13} = \left(N_\phi^{(t_i, t)} + \frac{\epsilon_2}{2} N_\pi^{(t_i, t)} \right) \mathcal{P}^{\phi\phi}(p; t_i) \int d \ln q \, \frac{d}{d\phi(t_i)} \left[N_{JK}^{(t_i, t)} \mathcal{P}^{JK}(q; t_i) \right], \quad (4.8)$$

in which we have also expanded the sum over I . To repeat, the emergence of a single derivative along the unperturbed trajectory is a consequence of adiabaticity in the long-wavelength field configuration. The field and velocity variations combine to produce a shift along the unperturbed trajectory at t_i . The (apparently) independent variations $\delta\phi$ and $\delta\pi$ are really parametrized by a single variable, $\phi(t_i)$.

The prefactor of the integral is proportional to the linear power spectrum of the long mode \mathbf{p} at the end of inflation, $\mathcal{P}_\zeta(p; t)_{\text{tree}}$. This can be obtained using the separate universe approach, with initial surface set either soon after horizon crossing for \mathbf{p} , or at some later time, e.g., during the non-attractor phase, provided the initial conditions are chosen appropriately. In Ref. [2] we computed $\mathcal{P}_\zeta(p; t)_{\text{tree}}$ in the case of ultra-slow-roll, and explicitly showed that these two different choices of initialization time led to equivalent results. In particular, for an adiabatic configuration at \mathbf{p} we have

$$\mathcal{P}_\zeta(p; t)_{\text{tree}} = \left(N_\phi^{(t_\circ, t)} + \frac{\epsilon_2}{2} N_\pi^{(t_\circ, t)} \right)^2 \mathcal{P}^{\phi\phi}(p; t_\circ)_{\text{tree}} = \left(\frac{dN^{(t_\circ, t)}}{d\phi(t_\circ)} \right)^2 \mathcal{P}^{\phi\phi}(p; t_\circ)_{\text{tree}}, \quad (4.9)$$

where $t_o \gtrsim t_p$ is an arbitrary initialization time. Substituting Eq. (4.9) in Eq. (4.8) with $t_o = t_i$, and defining the relative correction $\Delta\mathcal{P} \equiv \mathcal{P}_{12+13}/\mathcal{P}_{\text{tree}}$, we obtain

$$\Delta\mathcal{P}_\zeta(p; t)_{12+13} \equiv \frac{\mathcal{P}_\zeta(p; t)_{12+13}}{\mathcal{P}_\zeta(p; t)_{\text{tree}}} = \left(\frac{dN^{(t_i, t)}}{d\phi(t_i)} \right)^{-1} \int d\ln q \frac{d}{d\phi(t_i)} \left[N_{JK}^{(t_i, t)} \mathcal{P}^{JK}(q; t_i) \right]. \quad (4.10)$$

We must now evaluate the change in the bracket $[\dots]$ induced by a shift in its initial data. In order to assign wavenumbers to inflationary perturbations, and therefore define the spectrum $\mathcal{P}^{JK}(q)$, we must wait until inflation has ended, taken to occur on a uniform energy hypersurface at time t_{end} . The horizon scale at this time defines some physical scale, associated with comoving wavenumber $q_{\text{end}} = (aH)_{t_{\text{end}}}$. Looking backwards from this hypersurface, we assign wavenumbers to the perturbations generated during inflation by the rule

$$\ln \frac{q}{q_{\text{end}}} = -N_{\text{lookback}} + \mathcal{O}(\epsilon), \quad (4.11)$$

where $N_{\text{lookback}} > 0$ is the lookback time to the horizon exit point of the corresponding fluctuation.

At time t_i , when the background configuration is shifted in Eq. (4.10), the band of enhanced modes contributing to the peak has already been generated. The change induced by $d/d\phi(t_i)$ therefore corresponds to insertion or removal of a short segment of the trajectory, which changes the lookback time. It follows that the change in the bracket $[\dots]$, for the modes of interest, merely amounts to a relabelling of wavenumbers.

A change $\delta\phi(t_i)$ in the field configuration produces a change $-\delta\phi(t_i)/\phi'(t_i)$ in the duration of inflation. If this is positive (corresponding to insertion of a small trajectory segment), then the required relabelling must shift the assignment of perturbations to smaller wavenumbers. Therefore the necessary relabelling is

$$\delta \ln q = \frac{\delta q}{q} = \frac{\delta\phi(t_i)}{\phi'(t_i)} + \mathcal{O}(\delta\phi)^2, \quad (4.12)$$

where $\phi' = d\phi/dN$ represents the field derivative with respect to the number of e-folds. As explained above, this relabelling is q -dependent, even if the shift $\delta\phi(t_i)$ is q -independent. It follows that $d/d\phi(t_i)$ in Eq. (4.10) can be recast into a derivative with respect to $\ln q$,

$$\frac{d}{d\phi(t_i)} \left[N_{JK}^{(t_i, t)} \mathcal{P}^{JK}(q; t_i) \right] = \frac{1}{\phi'(t_i)} \frac{d}{d\ln q} \left[N_{JK}^{(t_i, t)} \mathcal{P}^{JK}(q; t_i) \right]. \quad (4.13)$$

The result is that we can rewrite Eq. (4.10) as

$$\Delta\mathcal{P}_\zeta(p; t)_{12+13} = \int_{q_{\text{min}}}^{q_{\text{max}}} d\ln q \frac{d}{d\ln q} \left[N_{JK}^{(t_i, t)} \mathcal{P}^{JK}(q; t_i)_{\text{tree}} \right], \quad (4.14)$$

where we have marked explicitly the limits of integration and reintroduced the “tree” label for the power spectrum.

Eq. (4.14) represents one of our main results. Before discussing its consequences, let us comment on what we believe is interesting about Eq. (4.14). The fundamental theorem of calculus relates integration to differentiation, in the sense that if $\int f(x) dx = F(x)$, then

$dF(x)/dx = f(x)$. Therefore it is hardly remarkable that the integral in Eq. (4.14) can be expressed as the antiderivative of *some* function $F(x)$. The useful feature is not the emergence of a total derivative *in itself*, but rather that we are able to identify this antiderivative explicitly. In particular, it is simply the combination $N_{JK}\mathcal{P}^{JK}(q)$.

4.2 Interpretation and discussion

To interpret Eq. (4.14) it will be helpful to refer to explicit examples of single-field models leading to enhanced short-scale fluctuations. As we have explained, this is typically achieved by inclusion of a transient non-attractor (“NA”) phase, during which the decaying mode of ζ is promoted to a rapidly growing mode on superhorizon scales.

Dynamics of this kind constitutes a sub-class of constant-roll (“CR”) inflation [66]. During constant roll, the Klein–Gordon equation is $\ddot{\phi}/(H\dot{\phi}) \approx \beta$, with constant β , and $\epsilon_2 \approx 2\beta$. When $\beta < -3/2$ ($\epsilon_2 < -3$) there is no attractor in phase space. In this regime, the curvature perturbation evolves according to

$$\zeta(k, N)_{k \ll aH} = c_1 + c_2 \int^N dN' \exp \left(- \int^{N'} dN'' (3 - \epsilon_1 + \epsilon_2) \right). \quad (4.15)$$

For $\epsilon_1 \ll 1$ and $\epsilon_2 < -3$, ζ displays exponential growth. For most potentials that have already been studied, the transient non-attractor constant-roll dynamics are characterized by $\epsilon_2 \leq -6$, with $\epsilon_2 = -6$ (equivalently $\beta = -3$) being ultra-slow-roll.

Note that for $\beta > -3/2$ ($\epsilon_2 > -3$), the constant-roll model has attractor behaviour, and ζ is frozen on superhorizon scales. For example, ordinary slow-roll corresponds to $\beta = 0$. To avoid confusion, in the following we will always specify the value of ϵ_2 when we label a phase of dynamics as constant-roll.

After the non-attractor constant-roll phase, we assume the background evolves smoothly into a subsequent period, which we label “A”. Although other options are possible, we take this to be the Wands dual of the non-attractor phase [56, 67, 68]. This is again a constant-roll phase, now characterized by a dynamical attractor in phase-space, which quenches the growth of perturbations. Eventually, inflation ends. The second slow-roll parameter in the “A” phase is $\epsilon_{2,A} = -6 - \epsilon_{2,NA}$, where $\epsilon_{2,NA}$ is the value of ϵ_2 in the non-attractor phase.

We select two examples of typical single-field models leading to enhanced fluctuations: a ultra-slow-roll model with $\epsilon_{2,NA} = -6$, and a constant-roll model with $\epsilon_{2,NA} = -7$. These are representative of generic non-attractor constant-roll models. The critical difference between these models is the value of ϵ_2 in the subsequent dual phase. For ultra-slow-roll, $\epsilon_{2,A} \approx 0$, while for constant-roll with $\epsilon_{2,NA} = -7$ one has $\epsilon_{2,A} \approx 1$.

To obtain numerical results we have used `PyTransport` [69] to implement the ultra-slow-roll model presented by Germani & Prokopec [70], which was adapted from García-Bellido & Ruiz Morales [71]. We have also implemented the constant-roll model introduced by Cicoli *et al.* [72]. For both models we make the same parameter choices used by Cole *et al.* [73]. In Fig. 1 we show the time-evolution of the first two slow-roll parameters for each model, and in Fig. 2 we show the corresponding tree-level scalar power spectrum computed at the end of inflation.

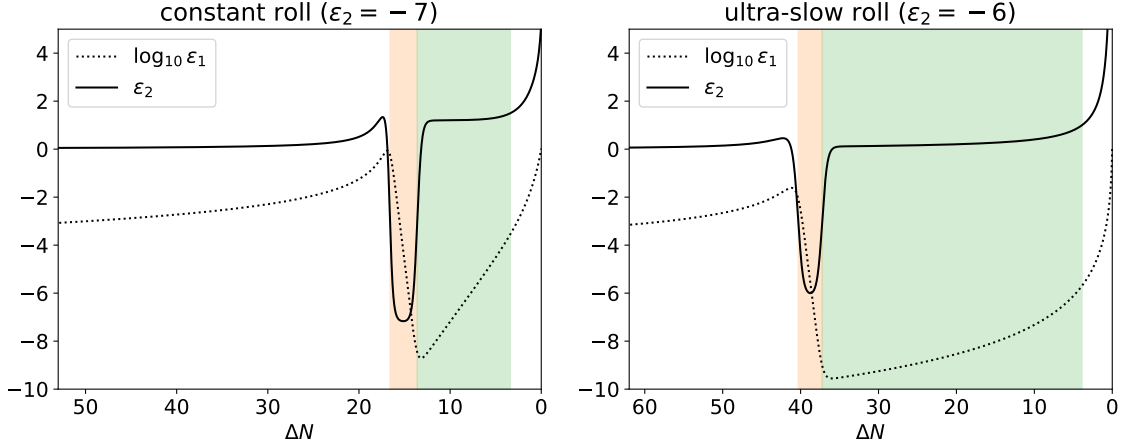


Figure 1: Time-evolution of ϵ_1 and ϵ_2 for two models leading to amplified fluctuations on small scales; see main text for details. In both panels the horizontal axis is $\Delta N \equiv N - N_{\text{end}}$, where N_{end} labels the end of inflation. We highlight times during the non-attractor phase ($\epsilon_2 < -3$) in orange, and the following dual attractor phase in green.

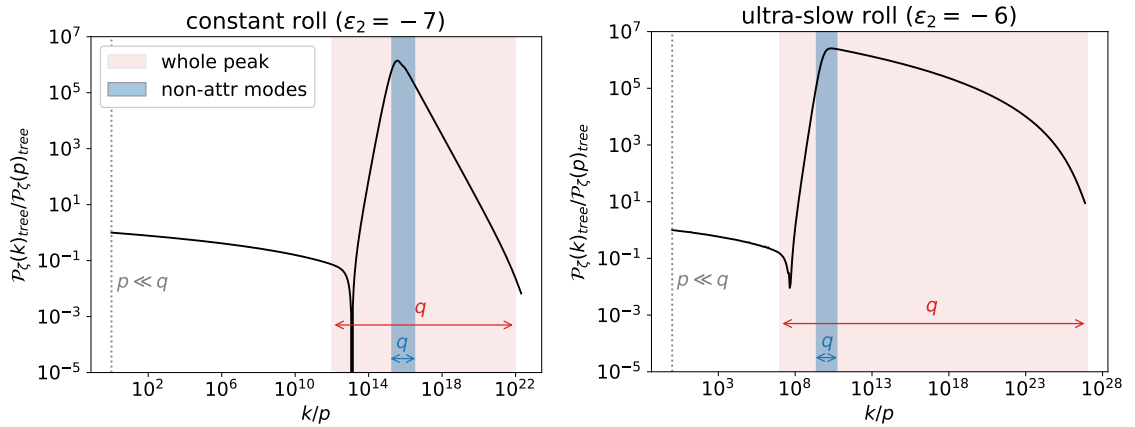


Figure 2: Tree-level scalar power spectrum $\mathcal{P}_\zeta(k)_{\text{tree}}$, for the models of Fig. 1; see main text for details. In both panels, the vertical dotted line identifies the long adiabatic mode p , for which we wish to estimate the back-reaction. Modes highlighted in blue cross the horizon during the non-attractor CR phase, defined by the condition $\epsilon_2 < -3$, as in Fig. 1. We label the first and last scale of the blue band as k_s and k_e , respectively. We highlight the broad peak in red.

Only the integral boundaries contribute.—Formally, one can use Eq. (4.14) to estimate the contribution to the 1-loop correction from the band of enhanced modes. This yields

$$\Delta\mathcal{P}_\zeta(p; t)_{12+13} = N_{JK}^{(t_i, t)} \mathcal{P}^{JK}(q; t_i)_{\text{tree}} \Big|_{q=q_{\max}} - N_{JK}^{(t_i, t)} \mathcal{P}^{JK}(q; t_i)_{\text{tree}} \Big|_{q=q_{\min}}. \quad (4.16)$$

We conclude that the contribution from this band can be expressed in terms of the phase-space power spectrum evaluated at its boundaries, q_{\min} and q_{\max} . The loop correction receives contributions from all modes with $q_{\min} \leq q \leq q_{\max}$, but it decouples from the precise details of their behaviour. In a full calculation, Eq. (4.16) would be accompanied by integrals over the infrared and ultraviolet regions that would subtract any dependence on q_{\min} and q_{\max} . In this sense these limits are arbitrary, but we can exploit this arbitrariness for the purpose of making an estimate.

As explained in §3.1, because our calculation is performed within the separate universe framework, we must choose the scale q_{\max} to be smaller than the inverse of the separate universe smoothing scale. Meanwhile, the scale q_{\min} can be any wavenumber sufficiently larger than p , i.e., $q_{\min} \gg p$. One possible choice is the first scale that crossed the horizon during the non-attractor phase, which we label k_s (see Fig. 2). To obtain the best estimate, in the sense of minimizing large subtractions from adjoining regions, we should choose q_{\min} and q_{\max} to bracket the whole enhanced band, represented by the red-shaded region in Fig. 2. In particular, we must choose the initial time t_i of §3.1 substantially later than the transition into the final slow-roll era, represented by the right-hand edge of the orange-shaded region in Fig. 1. We have already seen that this raises the possibility of a substantial loop correction to the (11) initial condition at t_i .

The case of a transient ultra-slow-roll phase.—In some models, further simplifications are possible. For the choices of initial time discussed above, the q -modes included in the loop integral are on superhorizon scales. Further, because t_i lies during an attractor phase, $\zeta_{\mathbf{q}}$ is constant, and therefore

$$\delta\phi_{\mathbf{q}} \propto \sqrt{\epsilon_1} \quad \text{and} \quad \delta\pi_{\mathbf{q}} = \frac{\epsilon_2}{2} \delta\phi_{\mathbf{q}} + \text{decaying}. \quad (4.17)$$

The relative importance of field and velocity fluctuations at t_i is determined by the second slow-roll parameter $\epsilon_2(t_i)$. Reference to the panels of Fig. 1 shows that, if the non-attractor phase is of ultra-slow-roll type, there is a period where $\epsilon_2(t_i) \approx 0$. (In the right-hand panel of Fig. 1 this matches most of the green region, excluding its right-hand edge where ϵ_2 is growing.) On the other hand, the left-hand panel of Fig. 1 shows that if the non-attractor phase is of constant-roll type, there is nowhere to locate t_i within the green region where $\epsilon_2(t_i)$ is negligible.

If it is possible to find a t_i for which $\epsilon_2(t_i)$ is sufficiently small, but where q_{\max} can still be chosen to bracket most of the enhanced band, then it is possible to simplify Eq. (4.16) by including only field fluctuations. In the right-hand panel of Fig. 1 this would correspond to choosing t_i somewhere near the middle of the green region. One could then not choose q_{\max} to cover the whole band of enhanced modes (see the corresponding panel of Fig. 1). However, $\mathcal{P}_\zeta(q_{\max}, t_i)$ would still be significantly smaller than its value at the peak. One would then have to accept the possibility of some cancellation with the ultraviolet region,

but presumably this is not an $O(1)$ effect. Accepting these limitations and setting $J = K = \phi$, we obtain

$$\Delta\mathcal{P}_\zeta(p; t)_{12+13} = \int_{q_{\min}}^{q_{\max}} d \ln q \frac{d}{d \ln q} \left[N_{\phi\phi}^{(t_i, t)} \mathcal{P}^{\phi\phi}(q; t_i)_{\text{tree}} \right] + O[\epsilon_2(t_i)]. \quad (4.18)$$

Where the $\epsilon_2(t_i)$ term can be neglected, it is possible to give a simple interpretation of the remaining integral. Since this seems mostly possible in ultra-slow-roll type scenarios, we will indicate this simplified version of Eq. (4.14) with a “USR” label.

After multiplying and dividing the function inside square brackets $[\dots]$ by $[N_\phi^{(t_i, t)}]^2$, it is possible to reconstruct the amplitude of the local bispectrum generated from non-linear evolution (which we label $f_{\text{NL}}^{N_{\phi\phi}}(k_i; t)$), and the short-scale scalar power spectrum, $\mathcal{P}_\zeta(q; t)_{\text{tree}}$. In particular,

$$\begin{aligned} \Delta\mathcal{P}_\zeta(p; t)_{12+13, \text{USR}} &\approx \int_{q_{\min}}^{q_{\max}} d \ln q \frac{d}{d \ln q} \left[\underbrace{\frac{N_{\phi\phi}^{(t_i, t)}}{N_\phi^{(t_i, t)}^2}}_{6f_{\text{NL}}^{N_{\phi\phi}}(k_i; t)/5} \underbrace{N_\phi^{(t_i, t)}^2 \mathcal{P}^{\phi\phi}(q; t_i)_{\text{tree}}}_{\mathcal{P}_\zeta(q; t)_{\text{tree}}} \right] \\ &= \frac{6}{5} \int_{q_{\min}}^{q_{\max}} d \ln q \frac{d}{d \ln q} \left[f_{\text{NL}}^{N_{\phi\phi}}(k_i; t) \mathcal{P}_\zeta(q; t)_{\text{tree}} \right], \end{aligned} \quad (4.19)$$

where the $O(\epsilon_2)$ contribution has been dropped. Here, k_i is the scale that crossed the horizon at time t_i . This yields a simple estimate in terms of $f_{\text{NL}}^{N_{\phi\phi}}$ and \mathcal{P}_ζ ,

$$\Delta\mathcal{P}_\zeta(p; t)_{12+13, \text{USR}} \approx \frac{6}{5} f_{\text{NL}}^{N_{\phi\phi}}(k_i; t) \left[\mathcal{P}_\zeta(q_{\max}; t)_{\text{tree}} - \mathcal{P}_\zeta(q_{\min}; t)_{\text{tree}} \right]. \quad (4.20)$$

If q_{\min} and q_{\max} adequately bracket the enhanced band, so that $\mathcal{P}_\zeta(q_{\max}; t)_{\text{tree}}$ and $\mathcal{P}_\zeta(q_{\min}; t)_{\text{tree}}$ are both substantially smaller than the peak amplitude (and we assume there is no large coupling with the ultraviolet portion of the integral) this represents a significant limitation on the importance of the 1-loop backreaction.

We close this discussion of the ultra-slow-roll case with a comment on the (13)-type loop. Applying the analysis of §4.1 to the (12)-type loop only, one obtains

$$\Delta\mathcal{P}_\zeta(p; t)_{12, \text{USR}} = N_{\phi\phi}^{(t_i, t)} \int d \ln q \frac{d}{d \ln q} \left[\mathcal{P}^{\phi\phi}(q; t_i) \right] + O[\epsilon_2(t_i)], \quad (4.21)$$

where again we have used (4.17) to neglect the contribution of momentum fluctuations. Now multiplying and dividing by a factor $N_\phi^{(t_i, t)}^2$, we obtain

$$\Delta\mathcal{P}_\zeta(p; t)_{12, \text{USR}} = \frac{6}{5} f_{\text{NL}}^{N_{\phi\phi}}(k_i; t) \int_{q_{\min}}^{q_{\max}} d \ln q \frac{d \mathcal{P}_\zeta(q; t)_{\text{tree}}}{d \ln q} + O[\epsilon_2(t_i)]. \quad (4.22)$$

Comparing Eqs. (4.20) and (4.22) shows that, where the $\epsilon_2(t_i)$ contribution can be neglected, the (13)-type loop itself can be at most of $O[\epsilon_2(t_i)]$. Notice that this does not at all imply the contribution of every 1-loop diagram with 13 topology is always of this order; in the language of non-equilibrium quantum field theory, these correspond to 1-loop diagrams mediated by

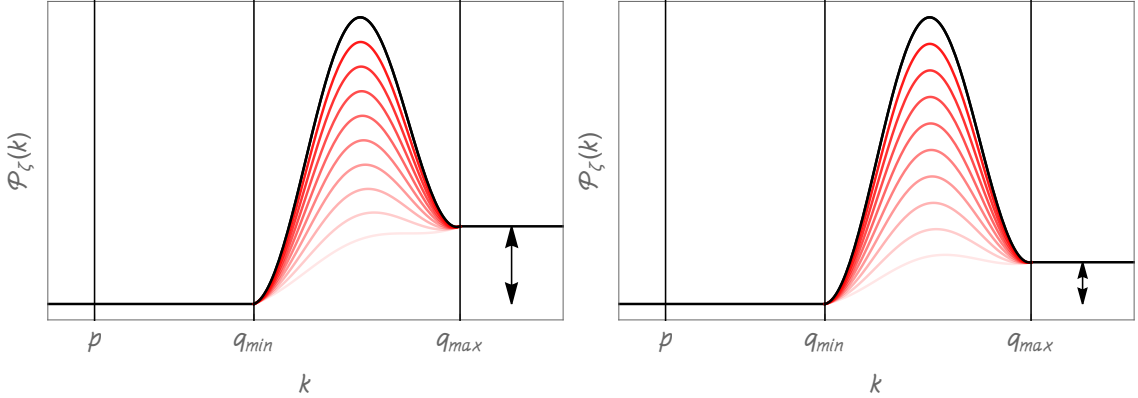


Figure 3: Schematic illustration of tree-level power spectra displaying a peak on short scales. These are not computed from realistic inflationary models (such as those in Fig. 2), but rather are toy examples. The vertical, black arrow indicates the (model-dependent) quantity $\mathcal{P}_\zeta(q_{\max}; t)_{\text{tree}} - \mathcal{P}_\zeta(q_{\min}; t)_{\text{tree}}$. In each panel, a reference spectrum is plotted in black. The red lines represent examples of other spectra with the same infrared and ultraviolet plateaus as the reference one, but with different amplitude of the peak.

one quartic interaction. Indeed, as we shall see in §5, the (11)-type loop in Eq. (3.16) includes a diagram with this topology, which does not need to be small.

Summary.—What should be concluded from Eqs. (4.16), (4.20) and (4.22)?

First, as explained above, the full 1-loop correction is independent of the limits q_{\min} and q_{\max} , which must be compensated by infrared and ultraviolet contributions that we have not written explicitly. To obtain the best estimate from (4.16), (4.20) and (4.22) we should choose q_{\min} and q_{\max} to minimize cancellations between these different contributions. As we have explained, this means that q_{\min} and q_{\max} should bracket the whole enhanced band. With these choices, and assuming the renormalization scale is at least modestly larger than q_{\max} , we should not expect large cancellations between the ultraviolet contribution and the estimate (4.16).

Second, given these choices for q_{\min} and q_{\max} , the major conclusion is that the amplitude of the 1-loop back-reaction decouples from all detailed properties of the central peak, including its maximum amplitude and width. See Fig. 3. It is not yet clear what is the spacetime picture of this decoupling, analogous to the picture of independent samples of q^{-1} -scale noise in a p^{-1} -scale region that leads to volume suppression of the (22)-type loop from the central limit theorem. For the case of (12)- and (13)-type diagrams, subtle correlations between the response of the short-scale fluctuations for different q combine to suppress the net backreaction. It would be interesting to understand this effect in terms of explicit realizations of the density field produced by such a power spectrum. Loosely speaking however, the long-wavelength description of the averaged short-scale mode would appear as an effective isocurvature mode. If the wavenumber- p field configuration is controlled by a theory that does not contain such a mode, it would not seem possible for the short-scale structure to excite one.

We note that there are longstanding results due to Senatore & Zaldarriaga [74] and Assassi *et al.* [42] showing that the correlation functions of ζ are constant to all orders in the loop expansion when inflation is of the single-clock variety. (See Senatore & Zaldarriaga [65, 75], and Pimentel *et al.* [76] for earlier related work.) Their results essentially amount to a demonstration that $d\hat{\zeta}_k/dt \rightarrow 0$ on superhorizon scales as an operator statement. Where these results apply, they prevent evolution of correlation functions when later substructure emerges from the horizon, and therefore prohibit back-reaction.

These results do not immediately apply to the scenario considered in this paper, for which the single-clock property does not have to hold during the non-attractor stage: we only have this property during the early and late attractor epochs. However, the details of our argument do not depend on the middle epoch being of non-attractor type, and they would continue to work if the enhanced band were produced by a single-clock scenario. (However, if this is the case, it is difficult to produce an enhancement of the kind required by PBH formation scenarios.) If the enhanced band is produced by a single clock phase, one can interpret our analysis as showing how the separate universe framework is compatible with the results of Senatore & Zaldarriaga and Assassi *et al.* If they are produced by a more general phase, our analysis is a generalization showing that adiabaticity (effectively the same as the single clock property) of the long-wavelength mode is sufficient, at least to 1-loop, irrespective of the short-scale substructure. In an effective description of the long-wavelength ζ field, it is attractive to interpret this result as a consequence of having no isocurvature modes that can be excited by the averaging procedure.

Third, the integral over the enhanced band does depend on the model, see the black arrow in the left and right panels of Fig. 3. Nevertheless, the entire effect is independent of the long-mode wavenumber p , as already noticed in Ref. [2]. Eq. (4.16) therefore represents a scale-invariant enhancement of the power spectrum amplitude, and it is not clear that the effect is observable. This model-dependence therefore does not translate into a constraint on individual scenarios.

5 The (11)-type loop is a boundary term

We now return to the possibility of a significant loop correction to the (11) initial condition. In order to compute it, we must be able to express the fields at t_i in terms of initial fields which have no back-reaction. This can be achieved by using an expansion method anchored before the transition into the non-attractor phase has taken place. The separate universe framework does not provide an appropriate method, because it would not allow the inclusion of all enhanced modes in the loop integrals. To discuss the (11)-type loop, we therefore consider the 1-loop computation in the context of a more general framework that does not rely on validity of the separate universe picture.

We continue to assume the properties of long and short modes described in §2. The discussion in §3.4 shows that, in the full framework of non-equilibrium field theory, we can model time evolution of the perturbations using the OPE-like expansion (3.19).¹⁰ In Con-

¹⁰The discussion in §3.4 shows that this is true up to 1-loop, which is all that is required for our present purposes. However, we expect that a similar statement can be made to all orders in the loop expansion.

stantini *et al.* [69], the Γ -tensors appearing as Wilson coefficients in this expansion were described as “multi-point propagators”, following the terminology of Bernardeau *et al.* [77]. As explained in §3.4, Eq. (3.19) is neither an approximation nor a model; it is equivalent to the full “in-in” formalism at 1-loop, provided all momentum-dependent effects are retained in the Γ coefficients, and the initial correlations are computed appropriately. It is therefore substantially more flexible than the separate universe framework, and in particular allows an arbitrary initial time, labelled t^* in Eq. (3.19). The price to be paid for this flexibility is a substantially more complex form of the Wilson coefficients, represented by the multi-point propagators. These propagators are scale-dependent objects and their interpretation is less straightforward than that of δN coefficients.¹¹

In §5.1 we show how multi-point propagators allow us to complete the δN 1-loop computation of §3, at least formally. Specifically, we use them to determine some properties of the initial condition for the (11)-type loop. This is sourced by contributions accumulated by the 2-point correlation functions of the long-mode from the onset of the non-attractor phase up to the initialization time t_i ; see Eq. (3.21). We find that the integrand of the (11)-type loop can be expressed as a total derivative of the tree-level short-scale phase-space power spectrum contracted with a 3-index multi-point propagator. In §5.2 and §5.3 we discuss the implications of this result for 1-loop back-reaction.

5.1 The (11)-type loop

The initial condition required for the (11)-type loop in Eq. (3.21) is the 2-point correlation function at 1-loop, evaluated at t_i . Below, we explain how this can be computed using the multi-point propagator method.

Multi-point propagators.—Multi-point propagators were defined at the 2-point level by Crocce & Scoccimarro (although not named as such) in the context of renormalized cosmological perturbation theory [78]. The generalization to all n , and the term *multi-point propagator*, were introduced by Bernardeau, Crocce & Scoccimarro [77]. Applied to a classical field X^I they can be regarded as momentum-dependent generalizations of the separate universe coefficients, and measure the correlation between some non-linear, evolved field and its values at early times. Taking $t^* < t$, the first three multi-point propagators would be defined by

$$\begin{aligned} \frac{\partial X_{\mathbf{k}_1}^I(t)}{\partial X_{\mathbf{k}_2}^J(t^*)} &\equiv \Gamma^I{}_J(k_1)^{(t^*,t)} \delta^{(3)}(\mathbf{k}_1 - \mathbf{k}_2), \\ \frac{\partial^2 X_{\mathbf{k}_1}^I(t)}{\partial X_{\mathbf{k}_2}^J(t^*) \partial X_{\mathbf{k}_3}^K(t^*)} &\equiv \Gamma^I{}_{JK}(k_1, k_2, k_3)^{(t^*,t)} \delta^{(3)}(\mathbf{k}_1 - \mathbf{k}_2 - \mathbf{k}_3), \\ \frac{\partial^3 X_{\mathbf{k}_1}^I(t)}{\partial X_{\mathbf{k}_2}^J(t^*) \partial X_{\mathbf{k}_3}^K(t^*) \partial X_{\mathbf{k}_4}^L(t^*)} &\equiv \Gamma^I{}_{JKL}(k_1, k_2, k_3, k_4)^{(t^*,t)} \delta^{(3)}(\mathbf{k}_1 - \mathbf{k}_2 - \mathbf{k}_3 - \mathbf{k}_4), \end{aligned} \quad (5.1)$$

¹¹A point of terminology: in a conventional OPE, the Wilson coefficients capture short-distance effects, whereas the operators in the expansion capture long-distance effects. In Eq. (3.19) we are allowing the Γ coefficients to stand in for operators with higher-derivatives. To obtain an OPE in the usual form we should expand each Γ as a Taylor series in its long-wavelength momenta. The coefficients of these series are the usual Wilson coefficients.

where t^* is an arbitrary initial time, as in Eq. (3.19). When applied to a quantum field \hat{X}^I , the notion of multi-point propagators as computable from derivatives would be lost, as for ordinary Wilson coefficients, and they would have to be obtained in some other way. We will see below that they obey evolution equations obtained from the Heisenberg equation of motion for \hat{X}^I , as explained in §3.4. In Ref. [62] the multi-point propagator expansion was introduced as a formal solution for the transport equations of inflationary correlations [60, 61, 63, 69, 79, 80].

Whether applied to a classical or quantum field, homogeneity and isotropy implies that Γ^I_J and Γ^I_{JK} depend only on the magnitude of their momentum labels. Each multi-point propagator is a bitensor, carrying a single momentum label (the first label) for the Fourier mode of the late-time field, followed by those corresponding to early-time phase-space variables. For the 2-index multi-point propagator Γ^I_J , the δ -function forces these momenta to have the same magnitude. (Therefore the 2-index propagator $\Gamma^I_J(k_1)$ carries just a single momentum label.) The argument of §3.4 determines the multi-point propagator expansion up to 1-loop in the 2-point function. Restoring explicit momentum labels, it is

$$\begin{aligned} X_{\mathbf{k}}^I(t) = & \Gamma^I_J(k)^{(t^*, t)} X_{\mathbf{k}}^J(t^*) + \frac{1}{2!} \int d^3 k_1 \Gamma^I_{JK}(k, k_1, |\mathbf{k} - \mathbf{k}_1|)^{(t^*, t)} X_{\mathbf{k}_1}^J(t^*) X_{\mathbf{k} - \mathbf{k}_1}^K(t^*) \\ & + \frac{1}{3!} \int d^3 k_1 \int d^3 k_2 \Gamma^I_{JKL}(\mathbf{k}, \mathbf{k}_1, \mathbf{k}_2, \mathbf{k} - \mathbf{k}_1 - \mathbf{k}_2)^{(t^*, t)} X_{\mathbf{k}_1}^J(t^*) X_{\mathbf{k}_2}^K(t^*) X_{\mathbf{k} - \mathbf{k}_1 - \mathbf{k}_2}^L(t^*) \\ & + \mathcal{O}(X^4). \end{aligned} \quad (5.2)$$

In Ref. [69] the multi-point propagator method was implemented numerically as an extension of the `PyTransport` package [81] for computation of 2- and 3-point correlators of ζ at tree-level. The implementation has advantages over the previous implementation, which calculated the evolution of each correlation function directly and was described in Ref. [60]. In particular, for topical ultra-slow-roll models, Ref. [69] found that, using the standard Runge–Kutta solver implemented in `PyTransport`, the multi-point propagator implementation can track the decay of correlations accurately for a longer period even when traditional `PyTransport` produces erroneous results. Also, it can obtain the bispectra in soft configurations for values of the squeezing parameter at least one decade beyond those attainable in the previous implementation. Moreover, as we shall demonstrate, the multi-point propagator expansion allows to construct correlators including loops. This is equivalent to use of transport equations directly for the phase-space correlators beyond tree-level, as discussed in §3.4.

Multi-point propagators in action: initial conditions for the (11)-type loop.—To proceed, we apply Eq. (5.2) to the perturbations $\delta X_{\mathbf{k}}^I$, and set initial conditions at time t^* just before the transition. This implies $t^* \lesssim t_{\text{tr}} \ll t_i$. In this configuration it seems safe to assume that the long-mode fields at time t^* are still unaffected by short scales, because these have not been displaced from their vacuum state. With this choice of initial conditions, we can represent a perturbation $\delta X_{\mathbf{p}}^I(t_i)$ using Eq. (5.2) with $\mathbf{k} = \mathbf{p}$, and $\mathbf{k}_1, \mathbf{k}_2$ replaced by two loop momentum labels \mathbf{q}, \mathbf{q}' .

The most important feature of Eq. (5.2) is that we can choose the initial time t^* to be *before* the onset of the non-attractor phase, whereas t_i continues to be set some time after

the last enhanced mode has crossed the horizon. We can therefore compute the (11)-loop in terms of the existing correlations at t^* and the Γ -coefficients. At time t^* , all of the modes that will later be enhanced by non-attractor dynamics are still in the subhorizon vacuum state. Notice that, in Eq. (5.2), no smoothing procedure is required or implied. Therefore, in principle, loop integrals built using it can include the contribution of modes up to an arbitrary ultraviolet scale.

Using Eq. (5.2) to evaluate the 2-point correlation function at t_i , we find three contributions: the (12)-, (22)-, (13)-type loops. We do not include a (11)-type loop, because we are assuming the fields at t^* have experienced no back-reaction and are still accurately Gaussian. All these contributions are topologically equivalent to the δN 1-loop diagrams listed in the right-hand-side of Eq. (3.16), and therefore we label them using the same convention. In the limit $p \ll q$, we find

$$\begin{aligned} P^{IJ}(p; t_i)_{12} &= \frac{1}{2} \int d^3q \alpha^{MNO}(p, q, q; t^*) \left[\Gamma_M^I(p)^{(t^*, t_i)} \Gamma_{NO}^J(p, q, q)^{(t^*, t_i)} + (I \leftrightarrow J) \right], \\ P^{IJ}(p; t_i)_{22} &= \frac{1}{2} \int d^3q \Gamma_{MN}^I(p, q, q)^{(t^*, t_i)} \Gamma_{OP}^J(p, q, q)^{(t^*, t_i)} P^{MO}(q; t^*) P^{NP}(q; t^*), \\ P^{IJ}(p; t_i)_{13} &= \frac{1}{2} \int d^3q P^{ML}(p; t^*) P^{NO}(q; t^*) \left[\Gamma_M^I(p)^{(t^*, t_i)} \Gamma_{LNO}^J(-\mathbf{p}, -\mathbf{p}, \mathbf{q}, -\mathbf{q})^{(t^*, t_i)} \right. \\ &\quad \left. + \Gamma_{MNO}^I(\mathbf{p}, \mathbf{p}, \mathbf{q}, -\mathbf{q})^{(t^*, t_i)} \Gamma_L^J(p)^{(t^*, t_i)} \right]. \end{aligned} \quad (5.3)$$

We now assume that the Γ -coefficients satisfy a soft theorem. Because the long mode provides a shifted background for the short scales, we can assume that the 4-index Γ needed for the (13)-type contribution is related to a shift in the 3-index Γ ,

$$\Gamma_{LNO}^J(-\mathbf{p}, -\mathbf{p}, \mathbf{q}, -\mathbf{q})^{(t^*, t_i)} \approx \frac{\partial}{\partial \delta X_{-\mathbf{p}}^L(t^*)} \Gamma_{NO}^J(-\mathbf{p}, \mathbf{q}, -\mathbf{q})^{(t^*, t_i)} \approx \frac{\partial}{\partial X^L(t^*)} \Gamma_{NO}^J(p, q, q)^{(t^*, t_i)}. \quad (5.4)$$

Under these assumptions, Eq. (5.4) follows from the properties of the long and short modes, described in §2. As a consequence, the 4-index Γ *in this specific case* depends only on the magnitude of its momenta. This property, together with symmetry of the long-mode power spectrum when it is evaluated much after horizon crossing (since we assume $t^* \gg t_p$), allows to rewrite the (13)-type loop in Eq. (5.3) as

$$P^{IJ}(p; t_i)_{13} = \frac{1}{2} \int d^3q P^{ML}(p; t^*) P^{NO}(q; t^*) \left[\Gamma_M^I(p)^{(t^*, t_i)} \Gamma_{LNO}^J(p, p, q, q)^{(t^*, t_i)} + (I \leftrightarrow J) \right]. \quad (5.5)$$

Now combining all contributions, we obtain

$$\begin{aligned} P^{IJ}(p; t_i)_{\text{1-loop}} &= P^{IJ}(p; t_i)_{12} + P^{IJ}(p; t_i)_{22} + P^{IJ}(p; t_i)_{13} \\ &= \frac{1}{2} \Gamma_M^I(p)^{(t^*, t_i)} \int d^3q \Gamma_{NO}^J(p, q, q)^{(t^*, t_i)} \alpha^{MNO}(p, q, q; t^*) + (I \leftrightarrow J) \\ &\quad + \frac{1}{2} \int d^3q \Gamma_{MN}^I(p, q, q)^{(t^*, t_i)} \Gamma_{OP}^J(p, q, q)^{(t^*, t_i)} P^{MP}(q; t^*) P^{NO}(q; t^*) \\ &\quad + \frac{1}{2} \Gamma_M^I(p)^{(t^*, t_i)} P^{ML}(p; t^*) \int d^3q \Gamma_{LNO}^J(p, p, q, q)^{(t^*, t_i)} P^{NO}(q; t^*) + (I \leftrightarrow J). \end{aligned} \quad (5.6)$$

Each Γ -coefficient must be regular in the limit $p \rightarrow 0$, otherwise the zero mode would diverge and represent an instability of the background. It follows that, in terms of the dimensionless power spectrum, the (22)-type diagram is suppressed for $p \rightarrow 0$.

Our discussion now parallels that of §4.1. We consider the sum of the remaining (12)- and (13)-type diagrams. Using the soft theorems (2.5) (for the squeezed bispectrum) and (5.4) (for the 4-index Γ), we obtain

$$\begin{aligned} \mathcal{P}^{IJ}(p; t_i)_{12+13} &= \Gamma_M^I(p)^{(t^*, t_i)} \mathcal{P}^{ML}(p; t^*) \int d^3 q \frac{\partial}{\partial X^L(t^*)} \left[\Gamma_{NO}^J(p, q, q)^{(t^*, t_i)} \mathcal{P}^{NO}(q; t^*) \right] \\ &\quad + (I \leftrightarrow J). \end{aligned} \quad (5.7)$$

Adiabaticity of the field configuration for the long mode means that the combination of partial derivatives appearing here can be replaced by a total derivative along the unperturbed trajectory, in the same way as Eqs. (4.7)–(4.8),

$$\begin{aligned} \mathcal{P}^{IJ}(p; t_i)_{12+13} &= \Gamma_M^I(p)^{(t^*, t_i)} \mathcal{P}^{M\phi}(p; t^*) \int d \ln q \frac{d}{d \phi(t^*)} \left[\Gamma_{NO}^J(p, q, q)^{(t^*, t_i)} \mathcal{P}^{NO}(q; t^*) \right] \\ &\quad + (I \leftrightarrow J). \end{aligned} \quad (5.8)$$

In the same way, the discussion of Eqs. (4.11)–(4.14) applies, enabling us to calculate the effect of a shift along the trajectory in terms of a relabelling of the short modes. Hence we can express the derivative $d/d\phi(t^*)$ in terms of $d/d \ln q$. These are all “soft limit” statements, which here we assume to be properties of correlation functions (evaluated at t^*) in the full non-equilibrium field theory.

The main result is that we conclude

$$\begin{aligned} \mathcal{P}^{IJ}(p; t_i)_{12+13} &= \Gamma_M^I(p)^{(t^*, t_i)} \mathcal{P}^{M\phi}(p; t^*) \frac{1}{\phi'(t^*)} \\ &\quad \times \int d \ln q \frac{d}{d \ln q} \left[\Gamma_{NO}^J(p, q, q)^{(t^*, t_i)} \mathcal{P}^{NO}(q; t^*) \right] + (I \leftrightarrow J). \end{aligned} \quad (5.9)$$

It follows that the (11)-type contribution given in Eq. (3.21) can be written

$$\begin{aligned} \mathcal{P}_\zeta(p; t)_{11} &= N_I^{(t_i, t)} N_J^{(t_i, t)} \left\{ \Gamma_M^I(p)^{(t^*, t_i)} \mathcal{P}^{M\phi}(p; t^*) \frac{1}{\phi'(t^*)} \right. \\ &\quad \left. \times \int d \ln q \frac{d}{d \ln q} \left[\Gamma_{NO}^J(p, q, q)^{(t^*, t_i)} \mathcal{P}^{NO}(q; t^*) \right] + (I \leftrightarrow J) \right\}. \end{aligned} \quad (5.10)$$

The conclusion is that the (11)-type loop correction must *also* formally have the structure of a total derivative, as a consequence of the multi-point propagator “OPE” Eq. (5.2) and the assumed soft-limit properties of the Γ coefficients with respect to the superhorizon mode \mathbf{p} . These are sufficient to show that the loop correction must organize itself into the form (5.10), regardless of the precise value of Γ_{NO}^J . In this sense, Eq. (5.10), and the analogous separate universe expression (4.14)—which can be regarded as a special case of the more general computation given here—can themselves be interpreted as soft limit theorems for the 1-loop contribution to the 2-point function in an adiabatic scenario.

5.2 Lessons from the loop computation

Neglecting loops that are suppressed in the $p \rightarrow 0$ limit, the 2-point function (3.16) for $\zeta_{\mathbf{p}}$ at 1-loop is

$$\mathcal{P}_\zeta(p; t)_{\text{1-loop}} = \mathcal{P}_\zeta(p; t)_{11} + \mathcal{P}_\zeta(p; t)_{12} + \mathcal{P}_\zeta(p; t)_{13}. \quad (5.11)$$

We computed $\mathcal{P}_\zeta(p; t)_{12} + \mathcal{P}_\zeta(p; t)_{13}$ in §4.1, and have just finished the computation of $\mathcal{P}_\zeta(p; t)_{11}$ in §5.1. Each contribution can be written in two ways, either in terms of a derivative with respect to the field configuration at time t^* or t_i , or in terms of the wavenumber q . For convenience we collect the final expressions below:

- total derivative in terms of the background field value:

$$\begin{aligned} \mathcal{P}_\zeta(p; t)_{11} &= N_I^{(t_i, t)} N_J^{(t_i, t)} \left\{ \Gamma^I{}_M(p)^{(t^*, t_i)} \mathcal{P}^{M\phi}(p; t^*) \right. \\ &\quad \left. \times \int_{q_{\min}}^{q_{\max}} d \ln q \frac{d}{d\phi(t^*)} \left[\Gamma^J{}_NO(p, q, q)^{(t^*, t_i)} \mathcal{P}^{NO}(q; t^*) \right] + (I \leftrightarrow J) \right\}, \end{aligned} \quad (5.12a)$$

$$\mathcal{P}_\zeta(p; t)_{12} + \mathcal{P}_\zeta(p; t)_{13} = N_I^{(t_i, t)} \mathcal{P}^{I\phi}(p; t_i) \int_{q_{\min}}^{q_{\max}} d \ln q \frac{d}{d\phi(t_i)} \left[N_{JK}^{(t_i, t)} \mathcal{P}^{JK}(q; t_i) \right]; \quad (5.12b)$$

- total derivative in terms of the loop comoving momentum q

$$\begin{aligned} \mathcal{P}_\zeta(p; t)_{11} &= N_I^{(t_i, t)} N_J^{(t_i, t)} \left\{ \Gamma^I{}_M(p)^{(t^*, t_i)} \mathcal{P}^{M\phi}(p; t^*) \frac{1}{\phi'(t^*)} \right. \\ &\quad \left. \times \int_{q_{\min}}^{q_{\max}} d \ln q \frac{d}{d \ln q} \left[\Gamma^J{}_NO(p, q, q)^{(t^*, t_i)} \mathcal{P}^{NO}(q; t^*) \right] + (I \leftrightarrow J) \right\}, \end{aligned} \quad (5.13a)$$

$$\mathcal{P}_\zeta(p; t)_{12} + \mathcal{P}_\zeta(p; t)_{13} = N_I^{(t_i, t)} \mathcal{P}^{I\phi}(p; t_i) \frac{1}{\phi'(t_i)} \int_{q_{\min}}^{q_{\max}} d \ln q \frac{d}{d \ln q} \left[N_{JK}^{(t_i, t)} \mathcal{P}^{JK}(q; t_i) \right]. \quad (5.13b)$$

The (11)-type loop exhibits the same structure as the (12)- and (13)-type loops, and can be given the same interpretation discussed in §4.2. We therefore reach the same conclusion, that the (11)-type contribution *also* decouples from the precise details of the enhanced band, and in particular from its maximum amplitude.

Clearly, there are examples in Nature where 1-loop contributions do not have the structure required by Eq. (5.13a). We therefore cannot expect this result to apply in general: there must be conditions under which it fails. In the argument given here, this occurs when the momentum configuration does not allow us to apply soft theorems to relate the 3- and 4-index Γ coefficients. Therefore, Eq. (5.13a) will not apply to (for example) loop corrections measured in terrestrial experiments, allowing us to recover the usual properties of quantum field theory in this regime.

We can now summarize our main messages.

- Given a suitable choice of initialization time for the separate universe framework, it is possible to choose q_{\min} , q_{\max} so that the loop correction adequately brackets a band of enhanced short-scale modes.
- Assuming suitable soft-limit properties for squeezed correlators or Γ -coefficients, the loop correction over the enhanced band organizes itself into a total derivative. It therefore decouples from the detailed properties of these modes. It follows that the amplitude of the loop correction will not be proportional to the amplitude at the peak.
- As already noted in Ref. [2], the loop integral over the enhanced band is scale invariant, and therefore not observable.

5.3 Renormalized δN coefficients

Before closing, we note that there is another way to understand a 1-loop formula such as Eq. (4.5) or Eq. (5.7). In this section, we show that the part of the 1-loop correction that is not volume-suppressed has a very simple interpretation as a *tree-level* correlation for a long-wavelength field obtained from a separate-universe expansion in a shifted background. This enables us to connect our analysis to a discussion of loops in the δN formalism given by Byrnes *et al.* [82].

In this section we return to the separate universe approach, and the analysis below is intended to apply only in this framework. The argument can be given for any perturbation. We give the discussion for $\zeta_{\mathbf{p}}$, but exactly the same procedure can be applied to any generic perturbation $\delta X_{\mathbf{p}}$. In the discussion of §4.1 we began with a large region of spacetime characterized by a background field configuration X_0^I and perturbations δX^I , as in Eq. (3.14). In Ref. [2] and §4.1 we evaluated corrections to $\langle \zeta_{\mathbf{p}} \zeta_{-\mathbf{p}} \rangle$ by building loops immediately from (3.15), and then identifying contributions from different regions of the loop momentum.

Byrnes *et al.* noticed that the expressions yielded by this procedure can be interpreted in terms of “renormalized” δN coefficients. To understand their result in our language, write the perturbations in the large region in the form $\delta X_{\text{total}}^I = \delta X_{<}^I + \delta X_{>}^I$, where the subscripts $<$, $>$ indicate that the field contains Fourier modes with wavenumbers $< p$ and $> p$, respectively. In the analysis of §4.1 we constructed separate universe expressions based on a Taylor expansion of $N(t)$ around the background X_0^I . This approach leads to expressions involving correlation functions of the total perturbation $\delta X_{\text{total}}^I$. We then identified the impact of $\delta X_{>}^I$ on correlations of $\delta X_{<}^I$ using the loop expansion as the primary tool.

An alternative strategy is to break the Taylor expansion of δN into two steps: first we make an expansion in $\delta X_{<}^I$ alone,

$$N = \tilde{N}_0 + \tilde{N}_I \delta X_{<}^I + \frac{1}{2!} \tilde{N}_{IJ} \delta X_{<}^I \delta X_{<}^J + \frac{1}{3!} \tilde{N}_{IJK} \delta X_{<}^I \delta X_{<}^J \delta X_{<}^K + \dots, \quad (5.14)$$

where the notation \tilde{N}_I , \tilde{N}_{JK} (and so on) indicates that each derivative is to be evaluated on the *shifted* field configuration $X_0^I + \delta X_{>}^I$. In a second step, we expand each \tilde{N} coefficient in terms of the short-scale fields $\delta X_{>}^I$. We then spatially average over these modes. This

is simply a reorganization of terms in the perturbation expansion, and so should yield an outcome equivalent to §4.1. We confirm this expectation explicitly below. Hence, for example,

$$\langle \tilde{N}_0 \rangle_> = N_0 + N_A \langle \delta X_>^A \rangle_> + \frac{1}{2!} N_{AB} \langle \delta X_>^A \delta X_>^B \rangle_> + \dots \quad (5.15)$$

$$\langle \tilde{N}_I \rangle_> = N_I + N_{IA} \langle \delta X_>^A \rangle_> + \frac{1}{2!} N_{IAB} \langle \delta X_>^A \delta X_>^B \rangle_> + \dots \quad (5.16)$$

On the right hand side we have written N_I , N_{IA} , N_{IAB} , because these derivatives are to be evaluated in the unshifted background and hence agree with the δN coefficients appearing in Eq. (3.15) and Eqs. (3.17a)–(3.17d). The brackets $\langle \dots \rangle_>$ indicate spatial averaging only over the $>$ fields. Similar formulas can be written for $\langle \tilde{N}_{IJ} \rangle_>$, $\langle \tilde{N}_{IJK} \rangle_>$ and all higher coefficients, but at 1-loop we do not need them.

We assume that $\langle \delta X_>^A \rangle_> = 0$. However, the short-scale variance $\langle \delta X_>^A \delta X_>^B \rangle_>$ can depend on the long wavelength field configuration on which it is evaluated. Therefore, assuming a suitable soft theorem,

$$\langle \delta X_>^A \delta X_>^B \rangle_> = \langle \delta X_>^A \delta X_>^B \rangle_>|_0 + \left(\frac{\partial}{\partial X_0^I} \langle \delta X_>^A \delta X_>^B \rangle_> \right) \Big|_0 \delta X_<^I + \dots, \quad (5.17)$$

where $|_0$ denotes evaluation in the unshifted background. Then it follows from Eq. (5.14) that

$$\begin{aligned} \langle N \rangle_> &= \left(N_0 + \frac{1}{2} N_{AB} \langle \delta X_>^A \delta X_>^B \rangle_> + \dots \right) \\ &+ \left(N_I + \frac{1}{2!} N_{AB} \frac{\partial}{\partial X_0^I} \langle \delta X_>^A \delta X_>^B \rangle_> + \frac{1}{2!} N_{IAB} \langle \delta X_>^A \delta X_>^B \rangle_> + \dots \right) \delta X_<^I \\ &\quad + \dots. \end{aligned} \quad (5.18)$$

The terms quadratic in $\delta X_<$ are not needed. These would be required for computation of the higher correlation functions, but not the 2-point function. We have dropped the subscript “0”s to reduce notational clutter; all coefficients in this expansion are intended to be evaluated without any shift of zero modes.

The conclusion is that $\zeta = \delta \langle N \rangle_>$ can be expressed in terms of $N(t)$, averaged over a shift in the background fields. (Notice that we shift the background field first, and then average. This is not the same as shifting the background field by the average $\langle \delta X_>^I \rangle$, which we have assumed to vanish.) Therefore ζ can be expressed in terms of a modified first-order coefficient, which Byrnes *et al.* described as “renormalized”. We denote such coefficients with a hat, viz. \hat{N}_I , \hat{N}_{IJ} , etc. Up to the 1-loop order considered here, we need only write $\zeta_< = \hat{N}_I \delta X_<^I + \dots$, where the renormalized coefficient \hat{N}_I satisfies

$$\hat{N}_I = N_I + \frac{1}{2!} N_{AB} \frac{\partial}{\partial X_0^I} \langle \delta X_>^A \delta X_>^B \rangle_> + \frac{1}{2!} N_{IAB} \langle \delta X_>^A \delta X_>^B \rangle_>. \quad (5.19)$$

Eq. (5.19) agrees with Eq. (25) of Ref. [82], except in that paper the fields were assumed to be Gaussian, and therefore the term involving the derivative of the two-point function was absent. This depends on long–short mode coupling and is needed to match the 3-point

contribution to the 1-loop formula (4.5). Notice that the derivative has to be correctly interpreted, as explained below.

To reproduce the 1-loop corrected 2-point function, Eq. (4.5), we compute

$$\langle \zeta_{<,\mathbf{p}} \zeta_{<,-\mathbf{p}} \rangle = \hat{N}_I \hat{N}_J \langle \delta X_{<,\mathbf{p}}^I \delta X_{<,-\mathbf{p}}^J \rangle. \quad (5.20)$$

The expected result follows immediately after expressing the spatial average $\langle \delta X_> \delta X_> \rangle_>$ in terms of the power spectrum,

$$\langle \delta X_>^A \delta X_>^B \rangle_> = \int_> \frac{d^3 q}{(2\pi)^3} P^{AB}(q) = \int_{q_{\min}}^{q_{\max}} d \ln q \mathcal{P}^{AB}(q). \quad (5.21)$$

To compute the $\partial/\partial X_0^I$ derivative appearing in Eq. (5.19) we should first compute the q -dependent response of $\mathcal{P}^{AB}(q)$ to a change in the zero mode, and then integrate this response over the relevant range of q . This procedure reproduces the formulae of §4.1.

Notice that this procedure does not reproduce the (22)-type loop. As explained in Ref. [2], this represents an average over short-scale noise uncorrelated with $\delta X_{<,\mathbf{p}}^I$, and hence cannot be absorbed into a renormalization of it. This term could be included, if desired, by allowing the “constant” first term on the right-hand side of Eq. (5.18) to have uncorrelated stochastic noise ξ . The 1-loop δN formula for the long-wavelength field would then become $\zeta = \hat{N}_I \delta X_<^I + \xi$, with $\langle \xi \xi \rangle$ reproducing the (22)-type contribution. This is very similar to renormalization of the matter density field by stochastic terms, as in the effective field theory of large scale structure, or renormalized halo bias.

As presented in Ref. [82] this argument was largely based on the combinatorics of Feynman-like diagrams. However, in this context it is easy to see that it has an interpretation in terms of back-reaction. The moral is that, to correctly compute correlations at wavenumber p , we should first replace N by its average $\langle N \rangle_>$ obtained by integrating over structure on shorter scales with wavenumbers $q \gg p$.

6 Discussion

In this paper, our intention was to determine the effect of enhanced short-scale perturbations on a large-scale, adiabatic field configuration produced by an (effectively) single-field inflationary model. The enhanced modes could be produced by a transient non-attractor phase during inflation, although the exact mechanism of enhancement is not important for our analysis. In this section, as in the rest of the paper, we use p to label the wavenumber of the large-scale mode, and q to denote a wavenumber associated with the enhanced short-scale band, with $p \ll q$.

Summary.—Initially, we work within the separate universe framework. Employing a δN formula for the long mode, and accounting for back-reaction due to short scales as in Ref. [2], we compute the power spectrum of $\zeta_{\mathbf{p}}$ up to and including 1-loop corrections. We initialize the separate universe computation shortly after the last enhanced mode leaves the horizon. With this choice we are able to include the entire band of enhanced modes. There are two contributions that are not volume-suppressed. The first type are due to non-linearities

in the δN formula, even if the perturbations δX^I that appear in it are themselves free of backreaction. These are the (12)- and (13)-type loop terms. The second type comes from back-reaction to the δX^I already at the initial time. At 1-loop level, the only relevant such term of this type is the (11)-loop; see Eq. (3.16).

The (11)-type contribution cannot be estimated using the separate universe framework, because it necessarily includes contributions from times when the back-reacting modes are close to the horizon scale. However, as explained in §5, it is possible to give an expression for it in terms of “multi-point propagators” or Γ coefficients. This technique has already been implemented (at tree level) in the `PyTransport` code for numerical evaluation of correlation functions during inflation [66]. It represents a possible approach to numerical evaluation of loop corrections. We expect to return to this issue in a future publication [59].

Using adiabaticity of the long-wavelength field configuration, and soft theorems for squeezed correlators and Γ coefficients, we show that the 1-loop correction organizes itself into a total derivative, as in Eqs. (5.12a)–(5.12b) and Eqs. (5.13a)–(5.13b). Specifically, the integral reduces to a boundary term involving a contraction of the short-scale (cross-) power spectrum with a suitable coefficient tensor.

In isolation, we cannot draw quantitative conclusions from this property, because these contributions must be accompanied by integrals over infrared (wavenumbers $< q_{\min}$ in the language of §4) and ultraviolet regions (wavenumbers $> q_{\max}$). These integrals must compensate for any q_{\min}, q_{\max} dependence of the result, because these are arbitrary scales and cannot appear in a physical prediction. However, if q_{\min}, q_{\max} bracket the whole of the enhanced band, we can expect the IR and UV integrals to depend only weakly on its presence, provided the renormalization scale is at least a little larger than q_{\max} . Notice that, if p is a typical CMB scale, we are implicitly choosing a renormalization scheme that is not tied to p .

For example, it is sometimes suggested that we can renormalize the 2-point function by matching to its observed amplitude $A_S^2 \sim 10^{-9}$ at the CMB pivot scale. This is certainly possible, but the renormalization scale is then far to the IR of the enhanced band. It follows that any effects associated with this band must be absorbed by the counterterms needed to define the 2-point function. Our calculation would be valid for a renormalization scheme that is independent of the enhanced band, for example by measuring masses associated with the inflationary sector on terrestrial scales $\sim q_{\text{ren}}$ where all wavenumbers are much larger than q_{\max} . For recent discussion of renormalization in the context of cosmological correlation functions, see Refs. [22, 29, 33, 83, 84] for ultra-slow-roll, and Refs. [85–88] for the case of slow-roll.

Eqs. (5.12a)–(5.12b) and (5.13a)–(5.13b) can be interpreted within the back-reaction model proposed in §1 of Iacconi *et al.* [2]. However, in that paper, we considered the back-reaction of a *single* enhanced mode onto the long-wavelength mode \mathbf{p} . In this paper we include (at least to the extent possible) the entire enhanced band. It is the aggregate effect of all these modes that decouples from their detailed properties, although the physical mechanism underlying this decoupling is not yet entirely clear. The conclusion is that a long-wavelength, adiabatic field configuration decouples from enhanced structure on short scales. This is very similar to the question posed in early work on the effective theory of

large-scale structure [89].¹² In that case, it was argued that the short-scale structure decoupled completely if it satisfied a virial condition. Here, the conclusion runs in the opposite direction, because we take the short-scale structure to be arbitrary. However, the condition of adiabaticity makes the long-wavelength field configuration special. In any case, as has been noted, the loop correction considered here is scale invariant, and therefore does not clearly have observable consequences. Similar conclusions have been reached by Tada *et al.* [14], Fumagalli [25] and Kawaguchi *et al.* [24] in the context of the full in-in framework.

We have also emphasized that decoupling of the short-scale structure seems to be necessary in an adiabatic scenario to maintain compatibility with calculations showing that the correlation functions of ζ are constant to all orders in the loop expansion in “single-clock” models, due to Senatore & Zaldarriaga [74] and Assassi *et al.* [42]. These papers both argue that, in such models and under rather general conditions, $d\hat{\zeta}_k/dt \rightarrow 0$ on superhorizon scales as an operator statement. (For earlier work, see Refs. [65, 75, 76].) In this paper we assume the single-clock property for the long wavelength modes, but not explicitly for the short ones, and we rely on a soft theorem to understand the response of the short-scale modes to the long-wavelength disturbance. Our analysis is therefore compatible with the conclusions of these papers, but generalizes the result to cases where the long wavelength field configuration is adiabatic, but the short modes are not.

(Non-)applicability of our results.—These results apply whenever our fundamental assumptions are satisfied. As explained in §2, these are: (1) adiabaticity of the long-wavelength field configuration, and (2) an appreciable hierarchy of scales, allowing application of soft theorems. A primary motivation for this scenario comes from the analysis of Kristiano & Yokoyama [5], who suggested that 1-loop back-reaction might invalidate conventional perturbation theory in models where enhanced small-scale structure produces a cosmologically-interesting abundance of primordial black holes. We interpret our result to show that, if the long-wavelength field configuration is adiabatic, then its statistical properties do not receive large renormalizations from the enhanced band.

Let us now discuss scenarios to which our results do *not* apply. First, our result should not be used to estimate the back-reaction of enhanced modes onto themselves. These modes are certainly not in an adiabatic configuration, because they are already evolving at tree-level. Further, there is no separation of scales. To study this kind of back-reaction, the separate universe framework loses all its advantages, and one would have to return to a formulation of the full non-equilibrium field theory. Firmly establishing the size of such “self”-corrections to the enhanced modes would be very important, because the phenomenology of models with non-attractor behaviour (such as production of primordial black holes or scalar-induced gravitational waves) is highly sensitive to the exact amplitude and scale dependence of the enhanced band. See Refs. [4, 90–93] for studies on 1-loop effects of enhanced small-scale

¹²Indeed, there are clear parallels between our back-reaction calculation and the effective field theory of large-scale structure. These are perhaps most clearly expressed in terms of the renormalized long-wavelength formula $\zeta = \hat{N}_I \delta X^I_< + \xi$ from §5.3. The main conclusions of §5.3 are that integrating out the short-wavelength modes introduces both additive and multiplicative renormalization of the tree-level operator $N_I \delta X^I_<$, with the multiplicative renormalization $N_I \rightarrow \hat{N}_I$ being introduced due to long–short correlations, and the stochastic term ξ being volume suppressed. These parallel equivalent conclusions in EFTofLSS [89].

modes at scales around the peak, and Ref. [94] for near-infrared scales.

Second, in the context of multiple-field inflationary models with active isocurvature perturbations, ζ may already evolve at tree-level on large scales after horizon exit. If this is the case, our results do not apply. Indeed, in the effective theory of the long-wavelength modes, one can presumably regard the averaged short-scale structure as exciting an effective isocurvature mode that drives evolution of ζ . We defer a full treatment of multiple-field models to future work.

Subtraction of squeezed initial conditions.—Before closing, we note one remaining technicality. Because soft theorems play a critical role in our analysis, our final formulae in §4 and §5 depend on the squeezed limit of correlation functions. Such squeezed configurations must be handled carefully. In particular, their physical content is not clear until an appropriate gauge transformation to physical coordinates is performed; see, e.g., Pajer *et al.* [95] and Tanaka *et al.* [96]. For the case of the tree-level bispectrum, this transformation amounts to subtraction of the leading term in Eq. (2.5).

In our analysis, we do not make such transformations, but work consistently on spatial hypersurfaces where the squeezed limit is not suppressed. In principle, we should perhaps make such a transformation *after* calculation of our loop, but this would not be expected to change the result for the 2-point function of p on observable scales. However, there is presumably an equivalent (perhaps simpler) description in which one works on physical hypersurfaces from the outset, and squeezed correlations are absent when the long-wavelength field configuration is adiabatic. This approach will presumably lead to the same conclusions obtained above. Techniques to perform the necessary subtractions were developed in the context of the separate universe framework by Tada & Vennin [97]. However, they have not yet been applied to loop calculations. We believe this is an important issue, to which we hope to return in future work.

Acknowledgments

LI is grateful to Guillermo Ballesteros, Matteo Braglia, Sebastián Céspedes, Jesús Gambín Egea, Arthur Poisson, Sébastien Renaux-Petel, as well as the participants to the workshops *Looping in the Primordial Universe* and *CoBALt* for interesting and useful discussions related to this work. DJM and LI are supported by the Science and Technology Facilities Council (grant number ST/X000931/1). DS is supported by the Science and Technology Facilities Council (grant number ST/X001040/1). For the purpose of open access, the authors have applied a Creative Commons Attribution (CC-BY) licence to any Author Accepted Manuscript version arising from this work.

A Tree-level application of separate universe to a ultra-slow-roll model

In this Appendix we explicitly show that separate universe was correctly implemented in Ref. [2] for a toy model featuring ultra-slow-roll (USR). To do so, we compute the linear scalar power spectrum, $\mathcal{P}_\zeta(k; t)_{\text{tree}}$, by starting a separate universe computation at time t_i

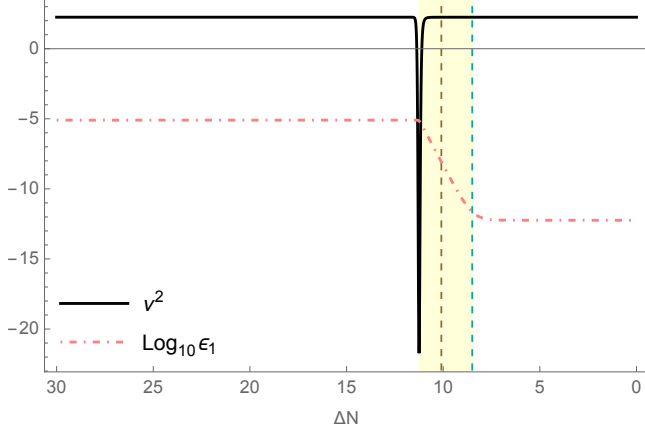


Figure 4: Evolution of the Mukhanov–Sasaki mass, ν^2 , and slow-roll parameter ϵ_1 , computed for the toy USR model analysed in Ref. [2]. On the horizontal axis we display the number of e-folds to the end of inflation, $\Delta N \equiv N_{\text{end}} - N$. The two vertical dashed lines mark the two choices of initialization time for the separate universe computations, $\eta_i = -1/k_{\text{peak}}$ (brown) and $\eta_i = -1/k_e$ (blue). The yellow region highlights USR evolution, defined by the condition $\epsilon_2 < -3$.

after the transition into USR has taken place. We consider two choices of t_i , (i) the horizon-crossing time of the peak scale, $t_i | k_{\text{peak}} = a(t_i)H$, and (ii) the end of USR, $t_i | k_e = a(t_i)H$. When expressed in terms of conformal time, these choices correspond to (i) $\eta_i = -1/k_{\text{peak}}$ and (ii) $\eta_i = -1/k_e$.

In Fig. 4 we display the time evolution of the first slow-roll parameter, ϵ_1 , and the Mukhanov–Sasaki mass,

$$\nu^2 = \frac{9}{4} - \epsilon_1 + \frac{3}{2}\epsilon_2 - \frac{1}{2}\epsilon_1\epsilon_2 + \frac{1}{4}\epsilon_2^2 + \frac{1}{2}\epsilon_2\epsilon_3 , \quad (\text{A.1})$$

computed for the USR model studied in Appendix A of Ref. [2]. One can see that after the initial transition into USR, ν^2 remains constant.

To compute $\mathcal{P}_\zeta(k; t)_{\text{tree}}$ we apply the strategy proposed in Ref. [43], see Appendix C therein. In particular, at time η_i we match the numerical solution to the Mukhanov–Sasaki equation for each mode $k < -1/\eta_i$ to its homogeneous counterpart, which provides the initial condition to describe the subsequent superhorizon evolution. Thanks to the semi-analytical nature of this method, at the time of the matching we discard gradient corrections and only include the homogeneous growing and decaying modes. We represent in Fig. 5 our results for $\mathcal{P}_\zeta(k; t)_{\text{tree}}$, which show excellent agreement with the numerical values. Note that all wavenumbers up to $k_i = -1/\eta_i$ (i.e. the inverse of the smoothing scale) are described correctly, including those which rise to the peak and those displaying scale-dependent oscillations around the peak.

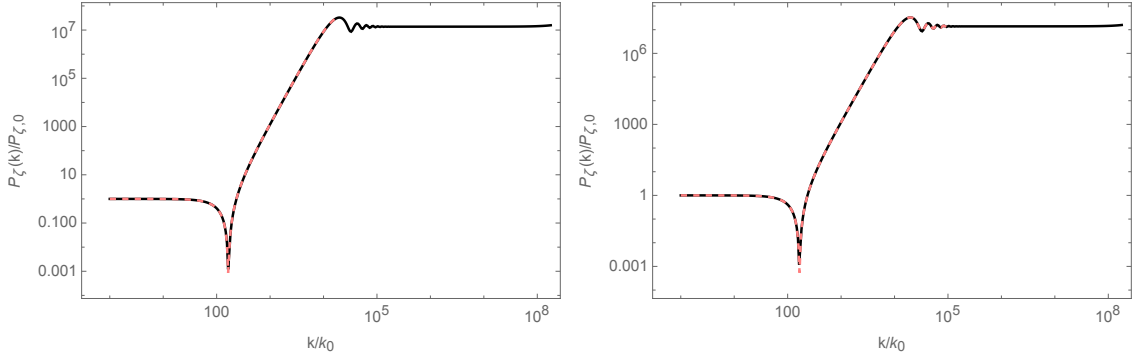


Figure 5: Linear power spectrum, $\mathcal{P}_\zeta(k; t)$ tree, computed by applying the separate universe approach (pink, dashed line), initialized at $\eta_i = -1/k_{\text{peak}}$ (left) and $\eta_i = -1/k_e$ (right). In both panels, the black line represents results obtained by numerically solving the Mukhanov–Sasaki equation.

B Squeezed phase-space bispectrum some e-folds after horizon crossing

In this Appendix, we compute the (tree-level) squeezed bispectrum $\alpha^{IJK}(p, q, q; t_i)$, which appears in Eq. (4.1) as the initial condition for the (12)-type δN loop.

Shortly after the scale q has crossed the horizon, the squeezed bispectrum can be estimated by soft-limit arguments, see Eq. (2.5). Nevertheless, in order to include the whole broadband of enhanced modes in our back-reaction estimate, t_i might be chosen substantially later than the horizon-crossing time of some q modes. Here, we employ the multi-point propagator expansion introduced in §5 to evaluate $\alpha^{IJK}(p, q, q; t_i)$, and determine how outside-the-horizon evolution between t_q and t_i contributes to the (12)-type loop in Eq. (4.1).

Note that since all modes involved are already superhorizon between t_q and t_i , the multi-point coefficients we employ are momentum independent. As a result, the expansion we use here is similar to the δN one, but formulated in phase space. For this reason, in the following we drop momentum labels when writing multi-point propagators.

By expanding phase-space fields at time t_i in terms of those at t_q , and substituting these in the 3-point correlator of interest, we find

$$\begin{aligned} \langle \delta X_{\mathbf{p}}^I \delta X_{\mathbf{q}}^J \delta X_{-\mathbf{p}-\mathbf{q}}^K \rangle_{t_i} &= \Gamma_M^I(t_q, t_i) \Gamma_N^J(t_q, t_i) \Gamma_O^K(t_q, t_i) \langle \delta X_{\mathbf{p}}^M \delta X_{\mathbf{q}}^N \delta X_{-\mathbf{p}-\mathbf{q}}^O \rangle_{t_q} \\ &+ \frac{1}{2} \Gamma_{MN}^I(t_q, t_i) \Gamma_O^J(t_q, t_i) \Gamma_P^K(t_q, t_i) \int d^3l \langle \delta X_{\mathbf{l}}^M \delta X_{\mathbf{p}-\mathbf{l}}^N \delta X_{\mathbf{q}}^O \delta X_{-\mathbf{p}-\mathbf{q}}^P \rangle_{t_q} \\ &+ \frac{1}{2} \Gamma_M^I(t_q, t_i) \Gamma_{NO}^J(t_q, t_i) \Gamma_P^K(t_q, t_i) \int d^3l \langle \delta X_{\mathbf{p}}^M \delta X_{\mathbf{l}}^N \delta X_{\mathbf{q}-\mathbf{l}}^O \delta X_{-\mathbf{p}-\mathbf{q}}^P \rangle_{t_q} \\ &+ \frac{1}{2} \Gamma_M^I(t_q, t_i) \Gamma_N^J(t_q, t_i) \Gamma_{OP}^K(t_q, t_i) \int d^3l \langle \delta X_{\mathbf{p}}^M \delta X_{\mathbf{q}}^N \delta X_{\mathbf{l}}^O \delta X_{-\mathbf{p}-\mathbf{q}-\mathbf{l}}^P \rangle_{t_q}. \end{aligned} \quad (\text{B.1})$$

Here, we have not yet taken the limit $p \ll q$. The first term encodes the linear evolution of the intrinsic phase-space bispectrum from t_q to t_i . The other three describe non-Gaussianity produced by non-linear super-horizon evolution between t_q and t_i . We note that higher-order contributions, e.g., those proportional to Γ_{JKL}^I , contribute beyond tree-level, and therefore have been neglected here.

After Wick contraction and taking the limit $p \ll q$, we obtain

$$\begin{aligned}\alpha^{IJK}(p, q, q; t_i) &= \Gamma_M^{I(t_q, t_i)} \Gamma_N^{J(t_q, t_i)} \Gamma_O^{K(t_q, t_i)} \alpha^{MNO}(p, q, q; t_q) \\ &+ \Gamma_{MN}^{I(t_q, t_i)} \Gamma_O^{J(t_q, t_i)} \Gamma_P^{K(t_q, t_i)} P^{MO}(q; t_q) P^{NP}(q; t_q) \\ &+ \Gamma_M^{I(t_q, t_i)} \Gamma_{NO}^{J(t_q, t_i)} \Gamma_P^{K(t_q, t_i)} P^{MO}(p; t_q) P^{NP}(q; t_q) \\ &+ \Gamma_M^{I(t_q, t_i)} \Gamma_N^{J(t_q, t_i)} \Gamma_{OP}^{K(t_q, t_i)} P^{MP}(p; t_q) P^{NO}(q; t_q).\end{aligned}\quad (\text{B.2})$$

Note we have used symmetry of the multi-point propagators under exchange of two lower indices. For later convenience, let us label each of the four terms as #1, #2, etc. We substitute Eq. (2.5) into #1, obtaining

$$\#1 = \Gamma_M^{I(t_q, t_i)} \Gamma_N^{J(t_q, t_i)} \Gamma_O^{K(t_q, t_i)} P^{MR}(p; t_q) \frac{\partial P^{NO}(q; t_q)}{\partial X^R(t_q)}. \quad (\text{B.3})$$

By applying the Leibniz rule, Eq. (B.3) can be rewritten as

$$\begin{aligned}\#1 &= \Gamma_M^{I(t_q, t_i)} P^{MR}(p; t_q) \frac{\partial}{\partial X^R(t_q)} \left[\Gamma_N^{J(t_q, t_i)} \Gamma_O^{K(t_q, t_i)} P^{NO}(q; t_q) \right] \\ &- \Gamma_M^{I(t_q, t_i)} P^{MR}(p; t_q) P^{NO}(q; t_q) \frac{\partial}{\partial X^R(t_q)} \left[\Gamma_N^{J(t_q, t_i)} \Gamma_O^{K(t_q, t_i)} \right].\end{aligned}\quad (\text{B.4})$$

In the first term one can switch the time of evaluation of the background field X^R in the derivative from t_q to t_i . This yields

$$\begin{aligned}\#1 &= \Gamma_M^{I(t_q, t_i)} P^{MR}(p; t_q) \Gamma_R^{S(t_q, t_i)} \frac{\partial}{\partial X^S(t_i)} \left[\Gamma_N^{J(t_q, t_i)} \Gamma_O^{K(t_q, t_i)} P^{NO}(q; t_q) \right] \\ &- \Gamma_M^{I(t_q, t_i)} P^{MR}(p; t_q) P^{NO}(q; t_q) \frac{\partial}{\partial X^R(t_q)} \left[\Gamma_N^{J(t_q, t_i)} \Gamma_O^{K(t_q, t_i)} \right].\end{aligned}\quad (\text{B.5})$$

In the first line, the contractions of Γ coefficients with $P^{MR}(p, t_q)$ and $P^{NO}(q, t_q)$ each produce a linearly evolved power spectrum at t_i . In the second line, the 2-index Γ symbols differentiate to a 3-index Γ symbol. As a result, we obtain (after relabelling summation indices)

$$\begin{aligned}\#1 &= P^{IS}(p; t_i) \frac{\partial P^{JK}(q; t_i)}{\partial X^S(t_i)} - \Gamma_M^{I(t_q, t_i)} \Gamma_{NO}^{J(t_q, t_i)} \Gamma_P^{K(t_q, t_i)} P^{MN}(p; t_q) P^{OP}(q; t_q) \\ &- \Gamma_M^{I(t_q, t_i)} \Gamma_N^{J(t_q, t_i)} \Gamma_{OP}^{K(t_q, t_i)} P^{MO}(p; t_q) P^{NP}(q; t_q).\end{aligned}\quad (\text{B.6})$$

Once #1 is combined with the other terms in Eq. (B.2), it can be seen that the second and third terms in Eq. (B.6) cancel with #3 and #4. Therefore, Eq. (B.2) reduces to

$$\begin{aligned}\alpha^{IJK}(p, q, q; t_i) &= P^{IS}(p; t_i) \frac{\partial P^{JK}(q; t_i)}{\partial X^S(t_i)} \\ &+ \Gamma_{MN}^{I(t_q, t_i)} \Gamma_O^{J(t_q, t_i)} \Gamma_P^{K(t_q, t_i)} P^{MO}(q; t_q) P^{NP}(q; t_q).\end{aligned}\quad (\text{B.7})$$

The first term has the same structure as Eq. (2.5), but is evaluated at t_i . The second term introduces a correction due to non-linear evolution between t_q and t_i , in which two short scales at t_q combine to produce a long mode at t_i .

The 1-loop correction to $\mathcal{P}_\zeta(p; t)$ induced by the second term in Eq. (B.7) is volume-suppressed in the limit of $p \rightarrow 0$. This can be seen by substitution in Eq. (4.1), which yields

$$\mathcal{P}_\zeta(p; t)_{12} \supset \frac{p^3}{2\pi^2} N_I^{(t_i, t)} N_{JK}^{(t_i, t)} \Gamma_{MN}^{(t_q, t_i)} \Gamma_O^{(t_q, t_i)} \Gamma_P^{(t_q, t_i)} \int d^3 q P^{MO}(q; t_q) P^{NP}(q; t_q) , \quad (B.8)$$

To conclude, we have shown that the squeezed bispectrum at t_i is given by two contributions, see Eq. (B.7). Of these, the second leads to volume-suppressed back-reaction, which justifies our use of Eq. (4.2) in §4.

References

- [1] A. Riotto, *The Primordial Black Hole Formation from Single-Field Inflation is Not Ruled Out*, [2301.00599](#).
- [2] L. Iacconi, D. Mulryne and D. Seery, *Loop corrections in the separate universe picture*, *JCAP* **06** (2024) 062 [[2312.12424](#)].
- [3] S.-L. Cheng, D.-S. Lee and K.-W. Ng, *Power spectrum of primordial perturbations during ultra-slow-roll inflation with back reaction effects*, *Phys. Lett. B* **827** (2022) 136956 [[2106.09275](#)].
- [4] K. Inomata, M. Braglia, X. Chen and S. Renaux-Petel, *Questions on calculation of primordial power spectrum with large spikes: the resonance model case*, *JCAP* **04** (2023) 011 [[2211.02586](#)].
- [5] J. Kristiano and J. Yokoyama, *Constraining Primordial Black Hole Formation from Single-Field Inflation*, *Phys. Rev. Lett.* **132** (2024) 221003 [[2211.03395](#)].
- [6] S. Choudhury, M. R. Gangopadhyay and M. Sami, *No-go for the formation of heavy mass Primordial Black Holes in Single Field Inflation*, *Eur. Phys. J. C* **84** (2024) 884 [[2301.10000](#)].
- [7] J. Kristiano and J. Yokoyama, *Note on the bispectrum and one-loop corrections in single-field inflation with primordial black hole formation*, *Phys. Rev. D* **109** (2024) 103541 [[2303.00341](#)].
- [8] A. Riotto, *The Primordial Black Hole Formation from Single-Field Inflation is Still Not Ruled Out*, [2303.01727](#).
- [9] H. Motohashi and Y. Tada, *Squeezed bispectrum and one-loop corrections in transient constant-roll inflation*, *JCAP* **08** (2023) 069 [[2303.16035](#)].
- [10] H. Firouzjahi and A. Riotto, *Primordial Black Holes and loops in single-field inflation*, *JCAP* **02** (2024) 021 [[2304.07801](#)].
- [11] G. Franciolini, A. Iovino, Junior., M. Taoso and A. Urbano, *Perturbativity in the presence of ultraslow-roll dynamics*, *Phys. Rev. D* **109** (2024) 123550 [[2305.03491](#)].
- [12] G. Tasinato, *Large $|\eta|$ approach to single field inflation*, *Phys. Rev. D* **108** (2023) 043526 [[2305.11568](#)].
- [13] J. Fumagalli, *Absence of one-loop effects on large scales from small scales in non-slow-roll dynamics*, *JHEP* **05** (2025) 162 [[2305.19263](#)].
- [14] Y. Tada, T. Terada and J. Tokuda, *Cancellation of quantum corrections on the soft curvature perturbations*, *JHEP* **01** (2024) 105 [[2308.04732](#)].

[15] S. Maity, H. V. Ragavendra, S. K. Sethi and L. Sriramkumar, *Loop contributions to the scalar power spectrum due to quartic order action in ultra slow roll inflation*, *JCAP* **05** (2024) 046 [[2307.13636](#)].

[16] H. Firouzjahi, *Revisiting loop corrections in single field ultraslow-roll inflation*, *Phys. Rev. D* **109** (2024) 043514 [[2311.04080](#)].

[17] M. W. Davies, L. Iacconi and D. J. Mulryne, *Numerical 1-loop correction from a potential yielding ultra-slow-roll dynamics*, *JCAP* **04** (2024) 050 [[2312.05694](#)].

[18] K. Inomata, *Superhorizon Curvature Perturbations Are Protected against One-Loop Corrections*, *Phys. Rev. Lett.* **133** (2024) 141001 [[2403.04682](#)].

[19] H. Firouzjahi, *Loop corrections in the bispectrum in ultraslow-roll inflation with PBHs formation*, *Phys. Rev. D* **110** (2024) 043519 [[2403.03841](#)].

[20] M. Braglia and L. Pinol, *No time to derive: unraveling total time derivatives in in-in perturbation theory*, *JHEP* **08** (2024) 068 [[2403.14558](#)].

[21] R. Kawaguchi, S. Tsujikawa and Y. Yamada, *Roles of boundary and equation-of-motion terms in cosmological correlation functions*, *Phys. Lett. B* **856** (2024) 138962 [[2403.16022](#)].

[22] G. Ballesteros and J. G. Egea, *One-loop power spectrum in ultra slow-roll inflation and implications for primordial black hole dark matter*, *JCAP* **07** (2024) 052 [[2404.07196](#)].

[23] J. Kristiano and J. Yokoyama, *Comparing sharp and smooth transitions of the second slow-roll parameter in single-field inflation*, *JCAP* **10** (2024) 036 [[2405.12145](#)].

[24] R. Kawaguchi, S. Tsujikawa and Y. Yamada, *Proving the absence of large one-loop corrections to the power spectrum of curvature perturbations in transient ultra-slow-roll inflation within the path-integral approach*, *JHEP* **12** (2024) 095 [[2407.19742](#)].

[25] J. Fumagalli, *Absence of one-loop effects on large scales from small scales in non-slow-roll dynamics. Part 2. Quartic interactions and consistency relations*, *JHEP* **01** (2025) 108 [[2408.08296](#)].

[26] J. Á. Ruiz and J. Rey, *Gravitational waves in ultra-slow-roll and their anisotropy at two loops*, *JCAP* **04** (2025) 026 [[2410.09014](#)].

[27] H. Firouzjahi, *Two-Loop Corrections in Power Spectrum in Models of Inflation with Primordial Black Hole Formation*, *Universe* **10** (2024) 456 [[2411.10253](#)].

[28] D. Frolovsky and S. V. Ketov, *One-loop corrections to the E-type α -attractor models of inflation and primordial black hole production*, *Phys. Rev. D* **111** (2025) 083533 [[2502.00628](#)].

[29] K. Inomata, *Conservation of superhorizon curvature perturbations at one loop: Backreaction in the in-in formalism and renormalization*, *Phys. Rev. D* **111** (2025) 103504 [[2502.08707](#)].

[30] C.-J. Fang, Z.-H. Lyu, C. Chen and Z.-K. Guo, *Incorporating backreaction in one-loop corrections in ultraslow-roll inflation*, *Phys. Rev. D* **112** (2025) 023547 [[2502.09555](#)].

[31] H. Firouzjahi and B. Nikbakht, *Non-Perturbative Hamiltonian and Higher Loop Corrections in USR Inflation*, [2502.09481](#).

[32] H. Firouzjahi and B. Nikbakht, *Hamiltonians to all Orders in Perturbation Theory and Higher Loop Corrections in Single Field Inflation with PBHs Formation*, [2502.10287](#).

[33] K. Inomata, *Role of the counterterms in the conservation of superhorizon curvature perturbations at one loop*, *Phys. Rev. D* **111** (2025) 123517 [[2502.12112](#)].

[34] W. H. Kinney, *Horizon crossing and inflation with large eta*, *Phys. Rev. D* **72** (2005) 023515 [[gr-qc/0503017](#)].

[35] K. Dimopoulos, *Ultra slow-roll inflation demystified*, *Phys. Lett. B* **775** (2017) 262 [[1707.05644](#)].

[36] C. Pattison, V. Vennin, H. Assadullahi and D. Wands, *The attractive behaviour of ultra-slow-roll inflation*, *JCAP* **08** (2018) 048 [[1806.09553](#)].

[37] J. M. Maldacena, *Non-Gaussian features of primordial fluctuations in single field inflationary models*, *JHEP* **05** (2003) 013 [[astro-ph/0210603](#)].

[38] Z. Kenton and D. J. Mulryne, *The squeezed limit of the bispectrum in multi-field inflation*, *JCAP* **10** (2015) 018 [[1507.08629](#)].

[39] Z. Kenton and D. J. Mulryne, *The Separate Universe Approach to Soft Limits*, *JCAP* **10** (2016) 035 [[1605.03435](#)].

[40] C. T. Byrnes, D. Regan, D. Seery and E. R. M. Tarrant, *The hemispherical asymmetry from a scale-dependent inflationary bispectrum*, *JCAP* **06** (2016) 025 [[1511.03129](#)].

[41] A. Kehagias and A. Riotto, *Operator Product Expansion of Inflationary Correlators and Conformal Symmetry of de Sitter*, *Nucl. Phys. B* **864** (2012) 492 [[1205.1523](#)].

[42] V. Assassi, D. Baumann and D. Green, *Symmetries and Loops in Inflation*, *JHEP* **02** (2013) 151 [[1210.7792](#)].

[43] J. H. P. Jackson, H. Assadullahi, A. D. Gow, K. Koyama, V. Vennin and D. Wands, *The separate-universe approach and sudden transitions during inflation*, *JCAP* **05** (2024) 053 [[2311.03281](#)].

[44] D. H. Lyth, *Non-gaussianity and cosmic uncertainty in curvaton-type models*, *JCAP* **06** (2006) 015 [[astro-ph/0602285](#)].

[45] A. A. Starobinsky, *Multicomponent de Sitter (Inflationary) Stages and the Generation of Perturbations*, *JETP Lett.* **42** (1985) 152.

[46] M. Sasaki and E. D. Stewart, *A General analytic formula for the spectral index of the density perturbations produced during inflation*, *Prog. Theor. Phys.* **95** (1996) 71 [[astro-ph/9507001](#)].

[47] D. Wands, K. A. Malik, D. H. Lyth and A. R. Liddle, *A New approach to the evolution of cosmological perturbations on large scales*, *Phys. Rev. D* **62** (2000) 043527 [[astro-ph/0003278](#)].

[48] D. H. Lyth and D. Wands, *Conserved cosmological perturbations*, *Phys. Rev. D* **68** (2003) 103515 [[astro-ph/0306498](#)].

[49] D. H. Lyth and Y. Rodriguez, *The Inflationary prediction for primordial non-Gaussianity*, *Phys. Rev. Lett.* **95** (2005) 121302 [[astro-ph/0504045](#)].

[50] M. Sasaki and T. Tanaka, *Superhorizon scale dynamics of multiscalar inflation*, *Prog. Theor. Phys.* **99** (1998) 763 [[gr-qc/9801017](#)].

[51] D. H. Lyth, K. A. Malik and M. Sasaki, *A General proof of the conservation of the curvature perturbation*, *JCAP* **05** (2005) 004 [[astro-ph/0411220](#)].

[52] V. Vennin and A. A. Starobinsky, *Correlation Functions in Stochastic Inflation*, *Eur. Phys. J. C* **75** (2015) 413 [[1506.04732](#)].

[53] J. M. Ezquiaga, J. García-Bellido and V. Vennin, *The exponential tail of inflationary fluctuations: consequences for primordial black holes*, *JCAP* **03** (2020) 029 [[1912.05399](#)].

[54] V. Briaud, R. Kawaguchi and V. Vennin, *Stochastic inflation with gradient interactions*, [2509.05124](#).

[55] M. Dias, R. H. Ribeiro and D. Seery, *The δN formula is the dynamical renormalization group*, *JCAP* **10** (2013) 062 [[1210.7800](#)].

[56] D. Wands, *Duality invariance of cosmological perturbation spectra*, *Phys. Rev. D* **60** (1999) 023507 [[gr-qc/9809062](#)].

[57] A. A. Starobinsky, *Spectrum of adiabatic perturbations in the universe when there are singularities in the inflation potential*, *JETP Lett.* **55** (1992) 489.

[58] D. H. Lyth and D. Seery, *Classicality of the primordial perturbations*, *Phys. Lett. B* **662** (2008) 309 [[astro-ph/0607647](#)].

[59] L. Iacconi, D. Mulryne and D. Seery, *in preparation*.

[60] M. Dias, J. Frazer, D. J. Mulryne and D. Seery, *Numerical evaluation of the bispectrum in multiple field inflation—the transport approach with code*, *JCAP* **12** (2016) 033 [[1609.00379](#)].

[61] G. J. Anderson, D. J. Mulryne and D. Seery, *Transport equations for the inflationary trispectrum*, *JCAP* **10** (2012) 019 [[1205.0024](#)].

[62] D. Seery, D. J. Mulryne, J. Frazer and R. H. Ribeiro, *Inflationary perturbation theory is geometrical optics in phase space*, *JCAP* **09** (2012) 010 [[1203.2635](#)].

[63] D. J. Mulryne, *Transporting non-Gaussianity from sub to super-horizon scales*, *JCAP* **09** (2013) 010 [[1302.3842](#)].

[64] M. Dias, J. Elliston, J. Frazer, D. Mulryne and D. Seery, *The curvature perturbation at second order*, *JCAP* **02** (2015) 040 [[1410.3491](#)].

[65] L. Senatore and M. Zaldarriaga, *On Loops in Inflation*, *JHEP* **12** (2010) 008 [[0912.2734](#)].

[66] H. Motohashi, *Constant-Roll Inflation*, 4, 2025, [2504.16757](#).

[67] H. Motohashi, A. A. Starobinsky and J. Yokoyama, *Inflation with a constant rate of roll*, *JCAP* **09** (2015) 018 [[1411.5021](#)].

[68] V. Atal and C. Germani, *The role of non-gaussianities in Primordial Black Hole formation*, *Phys. Dark Univ.* **24** (2019) 100275 [[1811.07857](#)].

[69] A. Costantini, L. Iacconi and D. J. Mulryne, *Primordial correlators from multi-point propagators*, *JCAP* **09** (2025) 077 [[2503.15194](#)].

[70] C. Germani and T. Prokopec, *On primordial black holes from an inflection point*, *Phys. Dark Univ.* **18** (2017) 6 [[1706.04226](#)].

[71] J. Garcia-Bellido and E. Ruiz Morales, *Primordial black holes from single field models of inflation*, *Phys. Dark Univ.* **18** (2017) 47 [[1702.03901](#)].

[72] M. Cicoli, V. A. Diaz and F. G. Pedro, *Primordial Black Holes from String Inflation*, *JCAP* **06** (2018) 034 [[1803.02837](#)].

[73] P. S. Cole, A. D. Gow, C. T. Byrnes and S. P. Patil, *Primordial black holes from single-field inflation: a fine-tuning audit*, *JCAP* **08** (2023) 031 [[2304.01997](#)].

[74] L. Senatore and M. Zaldarriaga, *The constancy of ζ in single-clock Inflation at all loops*, *JHEP* **09** (2013) 148 [[1210.6048](#)].

[75] L. Senatore and M. Zaldarriaga, *On Loops in Inflation II: IR Effects in Single Clock Inflation*, *JHEP* **01** (2013) 109 [[1203.6354](#)].

[76] G. L. Pimentel, L. Senatore and M. Zaldarriaga, *On Loops in Inflation III: Time Independence of zeta in Single Clock Inflation*, *JHEP* **07** (2012) 166 [[1203.6651](#)].

[77] F. Bernardeau, M. Crocce and R. Scoccimarro, *Multi-Point Propagators in Cosmological Gravitational Instability*, *Phys. Rev. D* **78** (2008) 103521 [[0806.2334](#)].

[78] M. Crocce and R. Scoccimarro, *Renormalized cosmological perturbation theory*, *Phys. Rev. D* **73** (2006) 063519 [[astro-ph/0509418](#)].

[79] D. J. Mulryne, D. Seery and D. Wesley, *Moment transport equations for non-Gaussianity*, *JCAP* **01** (2010) 024 [[0909.2256](#)].

[80] D. J. Mulryne, D. Seery and D. Wesley, *Moment transport equations for the primordial curvature perturbation*, *JCAP* **04** (2011) 030 [[1008.3159](#)].

[81] J. W. Ronayne and D. J. Mulryne, *Numerically evaluating the bispectrum in curved field-space— with PyTransport 2.0*, *JCAP* **01** (2018) 023 [[1708.07130](#)].

[82] C. T. Byrnes, K. Koyama, M. Sasaki and D. Wands, *Diagrammatic approach to non-Gaussianity from inflation*, *JCAP* **11** (2007) 027 [[0705.4096](#)].

[83] H. Sheikhahmadi and A. Nassiri-Rad, *Renormalized one-Loop Corrections in Power Spectrum in USR Inflation*, [2411.18525](#).

[84] J. Kristian and J. Yokoyama, *Inflationary background renormalization*, [2504.18514](#).

[85] G. Ballesteros, J. Gambín Egea and F. Riccardi, *Finite parts of inflationary loops*, *JHEP* **06** (2025) 098 [[2411.19674](#)].

[86] M. Braglia and L. Pinol, *One-loop renormalization of the effective field theory of inflationary fluctuations from gravitational interactions*, [2504.07926](#).

[87] M. Braglia and L. Pinol, *Freezing of the renormalized one-loop primordial scalar power spectrum*, [2504.13136](#).

[88] G. Ballesteros, J. G. Egea and F. Riccardi, *Finite parts of inflationary loops II: A streamlined UV in-in algorithm and distinguishable signatures*, [2512.20467](#).

[89] D. Baumann, A. Nicolis, L. Senatore and M. Zaldarriaga, *Cosmological Non-Linearities as an Effective Fluid*, *JCAP* **07** (2012) 051 [[1004.2488](#)].

[90] L. Iacconi and D. J. Mulryne, *Multi-field inflation with large scalar fluctuations: non-Gaussianity and perturbativity*, *JCAP* **09** (2023) 033 [[2304.14260](#)].

[91] A. Caravano, K. Inomata and S. Renaux-Petel, *Inflationary Butterfly Effect: Nonperturbative Dynamics from Small-Scale Features*, *Phys. Rev. Lett.* **133** (2024) 151001 [[2403.12811](#)].

[92] A. Caravano, G. Franciolini and S. Renaux-Petel, *Ultraslow-roll inflation on the lattice: Backreaction and nonlinear effects*, *Phys. Rev. D* **111** (2025) 063518 [[2410.23942](#)].

[93] A. Caravano, G. Franciolini and S. Renaux-Petel, *Ultraslow-roll inflation on the lattice. II. Nonperturbative curvature perturbation*, *Phys. Rev. D* **112** (2025) 083508 [[2506.11795](#)].

[94] J. Fumagalli, S. Bhattacharya, M. Peloso, S. Renaux-Petel and L. T. Witkowski, *One-loop infrared rescattering by enhanced scalar fluctuations during inflation*, *JCAP* **04** (2024) 029 [[2307.08358](#)].

[95] E. Pajer, F. Schmidt and M. Zaldarriaga, *The Observed Squeezed Limit of Cosmological Three-Point Functions*, *Phys. Rev. D* **88** (2013) 083502 [[1305.0824](#)].

- [96] T. Tanaka and Y. Urakawa, *Dominance of gauge artifact in the consistency relation for the primordial bispectrum*, *JCAP* **05** (2011) 014 [[1103.1251](#)].
- [97] Y. Tada and V. Vennin, *Squeezed bispectrum in the δN formalism: local observer effect in field space*, *JCAP* **02** (2017) 021 [[1609.08876](#)].